

Nearly sharp structured sketching for constrained optimization

Ke Chen* and Ruhui Jin*

October 21, 2020

Abstract

In this work, we study a tensor-structured random sketching matrix to project a large-scale convex optimization problem to a much lower-dimensional counterpart, which leads to huge memory and computation savings. We show that while maintaining the prediction error between a random estimator and the true solution with high probability, the dimension of the projected problem obtains optimal dependence in terms of the geometry of the constraint set. Moreover, the tensor structure and sparsity pattern of the structured random matrix yields extra computational advantage. Our analysis is based on probability chaining theory, which allows us to obtain an almost sharp estimate for the sketching dimension of convex optimization problems. Consequences of our main result are demonstrated in a few concrete examples, including unconstrained linear regressions and sparse recovery problems.

1 Introduction

Constrained optimization plays an important role in the intersection of machine learning [7], computational mathematics [31], theoretical computer science [8] and many other fields. We consider the least squares problem of the following form:

$$\mathbf{x}^* := \arg \min_{\mathbf{x} \in \mathcal{C}} \|\mathbf{A}\mathbf{x} - \mathbf{b}\|_2^2, \quad (1)$$

where $\mathcal{C} \subset \mathbb{R}^p$ is the convex constraint set, and $\mathbf{A} \in \mathbb{R}^{n \times p}$ and $\mathbf{b} \in \mathbb{R}^n$ are respectively the coefficient matrix and vector. When the optimal solutions are not unique, we denote $\mathbf{x}^* \in \mathbb{R}^p$ as one of the minimizers.

A naive approach to solve this over-determined problem (1) ($m \ll n$) requires polynomial time in the ambient dimension n , which is not ideal as n is remarkably high in large-scale optimization settings. *Sketching* is a leading alternative to approximate a high-dimensional system with lower-dimensional representations for less data memory, storage and computation complexity. It introduces a random matrix \mathbf{S} of size $m \times n$, called the sketching matrix, to reduce the original program (1) in a smaller problem:

$$\hat{\mathbf{x}} := \arg \min_{\mathbf{x} \in \mathcal{C}} \|(\mathbf{S}\mathbf{A})\mathbf{x} - (\mathbf{S}\mathbf{b})\|_2^2, \quad (2)$$

where the sketched coefficients $\mathbf{S}\mathbf{A}$, $\mathbf{S}\mathbf{b}$ are merely of m dimensions rather than n .

*Department of Mathematics, University of Texas, Austin, TX

In terms of error guarantees, we consider the following prediction error

$$\|\mathbf{A}\hat{\mathbf{x}} - \mathbf{b}\|_2^2 \leq (1 + \varepsilon)^2 \|\mathbf{A}\mathbf{x}^* - \mathbf{b}\|_2^2 \tag{3}$$

with high probability for a pre-specified error criterion $\varepsilon \in (0, 1)$. It is an interesting question how to design a sketching matrix \mathbf{S} with limited sketching dimension m that can achieve small prediction error in the sense of (3). This question has been well investigated in a line of work [17, 38, 29, 12, 3, 35, 36] based on common dimensionality reduction methods like CountSketch [9], sparse 0-1 matrices [14], Gaussian and sub-Gaussian matrices [39, 28], and FFT-based fast constructions [1, 44].

In many applications, the coefficient data \mathbf{A}, \mathbf{b} admit multi-linear (tensor) structures, for example in: spatio-temporal data analysis [4, 19], higher-order tensor decompositions [15, 24], approximating polynomial kernels [22, 34], linearized PDE inverse problems [10, 32] and so on. In the sketching setting, we can utilize the tensor structure in the original objective function to speed up forming the sketched problem by making the sketching matrix have a corresponding tensor structure. In this paper, we study the sketching matrix whose rows are tensor products of sub-Gaussian vectors. This design is natural to process the tensor data in the program. Previous works that share similar set-ups are [40, 10, 37]. We include the details of comparisons in later discussions.

Apart from the row-wise tensorized sketches, there are other multi-linear random projections and sampling strategies that work well in practice. For sketching constructions employing fast matrix-vector multiplications, Pagh et al. [33, 34] develop and analyze the TensorSketch method which uses fast Fourier transform (FFT) and CountSketch [9] techniques. This method is efficient while being applied to Kronecker products of vectors in the context of kernel machines. Later on, [16] provides applications of TensorSketch to Kronecker product regressions as well as multimodal p -spline tensor sketching. Another line of works is represented by [20, 26]. The authors respectively consider the so-called Kronecker FJLT. The analysis in both papers focuses on the subspace embedding property which can be seen as a stepping stone for sketching linear regressions. In the importance sampling regime, an efficient sublinear algorithm is provided by [11] to sample the tensor CP alternating least squares (CP-ALS) problem [24] by estimating the statistical leverage scores. [25] analyzes sparse sketching techniques in low-rank tensor regressions for tensor CP and Tucker decompositions. For computational advantage from the tensor structure in the sketching matrices, please see the works [10, 34, 20] for details.

The aforementioned previous works mostly rely on the Johnson-Lindenstrauss property [21] to embed pairwise distances and derive concentrations. While such strategy is easy to apply and powerful for subspace embedding, it falls short of capturing the essential dimension of a subset and thus is suboptimal in most constrained optimization problems. Recently, Pilanci et al. [35, 36] obtain sharp guarantees for constrained convex programs via the *Gaussian width* of the constraint set. Gaussian width is a widely used notion in learning theory, statistics and geometric analysis to estimate reconstruction errors of sub-Gaussian measurements [23, 5, 28]. It is capable of providing sharper bound than common concentration techniques like the union bound and ε -net [30].

1.1 Our contributions

The current work aims to capture the essential geometry of the constraint set in (1) and gain computational advantage from the tensor structure of the sketching matrix at the same time. In particular, our result adopts the same Gaussian width measure as in prior works [28, 35] and

extends the theory to tensorized sub-Gaussian cases. To the best of our knowledge, this paper presents the state-of-the-art sketching dimension for the row-wise tensor sketching matrices.

For the sake of simplicity of the exposition, we first present the main result Theorem 1.1 for the sketching design constructed with standard Gaussian¹ and Rademacher² vectors in the example of unconstrained linear regression problems. We would like to remark that a more comprehensive result later shown in Theorem 2.1 holds for a wide class of sub-Gaussian matrices with flexible density level and for all types of constrained least squares. For the proof of Theorem 1.1, we refer the readers to the proof of Theorem 2.1 shown in Section 3.2 and the proof of Corollary 2.2.

Theorem 1.1. *Let $n_1, n_2, p, m \in \mathbb{N}^+$. Consider the linear regression problem (1) ($n = n_1 n_2$) with coefficient matrix $\mathbf{A} \in \mathbb{R}^{n_1 n_2 \times p}$ and the constraint $\mathcal{C} = \mathbb{R}^p$. Fix the error criterion $\varepsilon \in (0, 1)$ and the failure probability $\delta \in (0, \frac{1}{2})$. Let $\mathbf{S} \in \mathbb{R}^{m \times n_1 n_2}$ be a sketching matrix such that each row of \mathbf{S} is an independent tensor product of a standard Gaussian vector of length n_1 and a Rademacher vector of length n_2 . If the sketching dimension m satisfies*

$$m = \mathcal{O} \left(\frac{\max(4 \operatorname{rank}(\mathbf{A}), |\log \delta|)}{\varepsilon^2} \right), \quad (4)$$

then the sketched solution $\hat{\mathbf{x}} \in \mathbb{R}^p$ in (2) satisfies the accuracy as in (3) with probability exceeding $1 - \delta$.

The estimate (4) indicates that for an unconstrained least squares Eq. (1) of large dimension n , one can obtain an accurate approximated solution with high probability by solving the sketched problem Eq. (2) of dimension m , which can be as small as $\mathcal{O}(\operatorname{rank}(\mathbf{A}))$. Our result (4) matches the result of the optimal unstructured sub-Gaussian sketching matrix in terms of their dependences on $\operatorname{rank}(\mathbf{A})$, ε and δ . We conclude that a row-wise tensor sketching strategy possesses both the computational advantage and the same accuracy as unstructured sketchings.

In addition, we manage to derive an estimate for constrained least squares, see Theorem 2.1. To this end, the generic chaining method is employed to bound the supreme embedding error over a convex cone generated by the true solution \mathbf{x}^* and the constraint set \mathcal{C} in (1). Such geometric description for constrained problems results in applications for various optimizations, such as ℓ_1 -constrained problems, see Corollary 2.3.

1.2 Related work

Sketching designs of row-wise tensor structure are previously studied in [40, 10, 37] with applications for data memory reductions, tensor decompositions and linear inverse problems. Through the lens of unconstrained linear regressions, by applying a standard covering net technique, their results are suboptimal. The sketching sizes m in the mentioned works are bounded below by $\operatorname{rank}^8(\mathbf{A})$, $\operatorname{rank}^6(\mathbf{A})$, $\operatorname{rank}^4(\mathbf{A})$ respectively for a qualified sketching to the linear regression in (1). Our work improves the estimate of m to a linear dependence on the rank of \mathbf{A} .

A similar construction of the sketching matrix is considered in Meister et al. [27], in which they form the sketching as the composition of a tensorized Rademacher matrix and a sparse $\{0, \pm 1\}$ -valued random matrix called CountSketch [9]. Compared to their sketching design, the construction of \mathbf{S} in this work considers a wider class of sub-Gaussian random variables. Moreover,

¹A standard Gaussian vector has i.i.d. $\mathcal{N}(0, 1)$ entries.

²A random Rademacher vector has i.i.d. entries which take the values $-1, 1$ with equal probability $1/2$.

our construction is easy to implement with adjustable sparsity. In terms of accuracy, the authors of [27] show their design is nearly optimal in vector-based embeddings. Particularly, by applying their result to the context of subspace embedding, their work gives a necessary lower bound of the sketching dimension

$$m \geq \max \left(\mathcal{O} \left(\frac{\text{rank}(\mathbf{A}) + |\log \delta \varepsilon|}{\varepsilon^2} \right), \mathcal{O} \left(\frac{\text{rank}^2(\mathbf{A}) + |\log \delta \varepsilon|^2}{\varepsilon} \right) \right), \quad (5)$$

to restrict the sketching error ε in the sense of (3) with probability $1 - \delta$. The estimate is shown to be optimal for their specific sparse sketching but unknown for other dense matrices. In comparison, we introduce a density level parameter q to adjust the number of nonzeros in the sketching matrix. In addition, our estimate $\max \left(\mathcal{O} \left(\frac{\text{rank}(\mathbf{A})}{\varepsilon^2 q^2} \right), \mathcal{O} \left(\frac{|\log \delta|}{\varepsilon^2 q} \right) \right)$ derived from Corollary 2.2 is able to match the first term in (5) in small ε regime, if setting the density q as a constant. In the large ε regime, it can be shown that our result can match the second term in (5), if we choose q larger than $\min \left(\frac{1}{\sqrt{\varepsilon \text{rank}(\mathbf{A})}}, \frac{1}{\varepsilon |\log \delta \varepsilon|} \right)$.

1.3 Notations

In the paper, we denote by $\| \cdot \|_2$ and $\| \cdot \|_\infty$ respectively the ℓ_2 and ℓ_∞ norms of a vector \mathbf{y} , and $\| \cdot \|$, $\| \cdot \|_F$ respectively the spectral and Frobenius norm of a matrix. The symbol \Pr denotes the probability of an event, and the notion \mathbb{E} is the expectation of a random variable. A n -dimensional vector following the distribution $\text{Ber}(q)^n$ has independent $\{0, 1\}$ -valued entries which take the value 1 with probability q . We use the calligraphic font \mathcal{X} to denote vector sets, the Roman script uppercase letter \mathbf{X} to denote matrices, the Roman script lowercase letter \mathbf{x} to denote vectors, and simple lowercase letter x to denote a scalar entry. We write $\mathbf{I}_n \in \mathbb{R}^{n \times n}$ as the n by n identity matrix. We denote $c, \tilde{c}, C_1, C_2, C', C''$ some universal absolute constants. The usage of the constant notations are consistent throughout the paper.

1.4 Organization of the paper

The rest of the paper is organized as follows. Section 2 starts with the reasoning for the sketching design and follows the main result Theorem 2.1 about the sketching dimension estimation, along with direct applications for two common classes of optimization problems. In Section 3, we show an important intermediate result Theorem 3.1 about the supremum embedding error of the tensorized processes and give the complete proof of Theorem 2.1 which is essentially built upon Theorem 3.1. The key ingredients and a simplified proof for Theorem 3.1 are then illustrated in Section 4. Section 5 contains the numerical performance of the proposed sketching construction and provides empirical support for the theory. We conclude and mention the future research directions in Section 6. The major volume of the technical proofs of this paper, including the proofs for all the supporting results shown in Section 4, are in the appendix.

2 Sketching dimension estimation

The main goal of the paper is to develop a sketching size estimation for the constrained least squares (2). In this section, we first introduce the tensor data structure in two examples as the motivation of our sketching matrix design. We present the main result Theorem 2.1 on a

nearly sharp sketching dimension bound in Section 2.2. We conclude this section with classical optimization cases as direct results of the main theorem.

We begin with some linear algebra and probability background.

Definition 2.1. Given matrices $\mathbf{X} \in \mathbb{R}^{M_1 \times N_1}$ and $\mathbf{Y} \in \mathbb{R}^{M_2 \times N_2}$, the Kronecker product of \mathbf{X} and \mathbf{Y} is defined as

$$\mathbf{X} \otimes \mathbf{Y} = \begin{bmatrix} x_{1,1}\mathbf{Y} & x_{1,2}\mathbf{Y} & \dots & x_{1,N_1}\mathbf{Y} \\ \vdots & \vdots & \ddots & \vdots \\ x_{M_1,1}\mathbf{Y} & x_{M_1,2}\mathbf{Y} & \dots & x_{M_1,N_1}\mathbf{Y} \end{bmatrix} \in \mathbb{R}^{M_1 M_2 \times N_1 N_2}. \quad (6)$$

The Kronecker product satisfies the distributive property:

$$\mathbf{W}\mathbf{X} \otimes \mathbf{Y}\mathbf{Z} = (\mathbf{W} \otimes \mathbf{Y})(\mathbf{X} \otimes \mathbf{Z}). \quad (7)$$

Assuming $M_1 = M_2$ and $N_1 = N_2$, the Hadamard product is defined as

$$\mathbf{X} \circ \mathbf{Y} \in \mathbb{R}^{M_1 \times N_1}, \quad (8)$$

which is the element-wise product of the matrices.

Definition 2.2. The sub-Gaussian norm of a random variable $x \in \mathbb{R}$, denoted by $\|x\|_{\psi_2}$, is defined as:

$$\|x\|_{\psi_2} = \inf\{t > 0 : \mathbb{E} \exp(x^2/t^2) \leq 2\}.$$

A random variable is sub-Gaussian if it has a bounded ψ_2 norm.

We note that all normal random variables and all bounded r.v.s are sub-Gaussian r.v.s.

Definition 2.3. Given a set $\mathcal{Y} \subset \mathbb{R}^n$, we use $\overline{\mathcal{Y}}$ to denote the normalized version of \mathcal{Y} :

$$\overline{\mathcal{Y}} = \left\{ \frac{\mathbf{y}}{\|\mathbf{y}\|_2} \in \mathbb{R}^n \mid \text{for } \mathbf{y} \in \mathcal{Y} \subset \mathbb{R}^n \right\}.$$

We define the Gaussian width of $\overline{\mathcal{Y}}$ as:

$$w(\overline{\mathcal{Y}}) = \mathbb{E} \sup_{\mathbf{y} \in \overline{\mathcal{Y}}} \langle \mathbf{n}, \mathbf{y} \rangle, \quad (9)$$

where $\mathbf{n} \in \mathbb{R}^n$ is a sequence of independent standard normal variables.

2.1 Design of the sketching matrix

Tensor structure is ubiquitous in applied mathematics [24], statistics [2] and deep learning [13]. Many datasets are naturally arranged with several attributes and can be represented as multi-arrays, namely tensors. Such structure also appears in the optimization problem (1) in practical applications. We initiate our sketching matrix design with two motivating examples: CANDECOMP/PARAFAC (CP) tensor decomposition and linearized PDE inverse problems.

CP tensor decomposition is an important tool for large-scale data analysis. The workhorse algorithm in fitting CP tensor decomposition is the alternating least squares, which solves the following convex optimization problem:

$$\arg \min_{\mathbf{X} \in \mathbb{R}^{R \times n}} \|\mathbf{A}\mathbf{X} - \mathbf{B}\|_F, \quad (10)$$

where \mathbf{A} and \mathbf{B} are data matrices that are flattened from certain tensors. The flattening process forces columns of \mathbf{A} to have tensor structures. In particular, let \mathbf{a} be a column of \mathbf{A} , then it can be rewritten as a Kronecker product:

$$\mathbf{a} = \bigotimes_{\ell=1}^d \mathbf{a}^{(\ell)},$$

where $d + 1$ is the order of the original tensor from which \mathbf{A} is unfolded. Due to the high computation cost of solving (10), sketching is used as a tool of solving CP tensor decomposition, see [6]. To relate the example to our work, we consider the $d = 2$ case.

Another interesting example is the class of linearized PDE inverse problems. One famous case is the Electrical Impedance Tomography (EIT), which infers the body conductivity images from boundary measurements of voltage and current density on the surface. The EIT problem generates the Fredholm equation of the kind:

$$\int f_{i_1}(y) g_{i_2}(y) \sigma(y) dy = \text{data}_{i_1, i_2}, \quad \forall 1 \leq i_1 \leq n_1, 1 \leq i_2 \leq n_2. \quad (11)$$

Here y is the spatial variable and σ is the image to reconstruct. The functions f_{i_1}, g_{i_2} are known from physical understanding of EIT, and data_{i_1, i_2} are observed data. The subscript i_1 and i_2 are indices for where the voltage is applied on the body surface and where the current is measured. In practice, one has to place electric nodes y_j on various places to produce sufficient data for the reconstruction, leading to a large number of equations with the same structure as in (11). A numerical discretization of (11) then produces a linear equation $\mathbf{A}\mathbf{x} = \mathbf{b}$, where $a_{i,j} = f_{i_1}(y_j) g_{i_2}(y_j)$, $x_j = \sigma(y_j)$, $b_i = \text{data}_{i_1, i_2}$ and the index i is associated with a pair of indices (i_1, i_2) . The above over-determined system is usually solved as an optimization problem (1). Each entry of \mathbf{A} is a product of functions f_{i_1} and g_{i_2} , and entries in one column share the same dependence on the spatial variable y_j . Due to this, it can be shown that such data structure is equivalent to having Kronecker structure for all columns of \mathbf{A} , that is, a column \mathbf{a} in \mathbf{A} can be written as:

$$\mathbf{a} = \mathbf{f} \otimes \mathbf{g} \in \mathbb{R}^{n_1 n_2}$$

for some column vectors $\mathbf{f} \in \mathbb{R}^{n_1}$ and $\mathbf{g} \in \mathbb{R}^{n_2}$. For more details of tensor structures in linearized inverse problem, we refer the readers to [10].

In the aforementioned examples, we see that tensor structure appears in the the columns of input matrix \mathbf{A} in the least squares objectives. When implementing the sketching strategy on the data matrix, the cost of the matrix multiplication $\mathbf{S}\mathbf{A}$ can be drastically reduced, if \mathbf{S} has a consistent tensor structure in its rows, due to the distributive property of Kronecker product (7). To further reduce the time complexity, we consider the sketching constructed with only a portion of nonzero entries. To this end, we design the sketching matrix \mathbf{S} in the following form:

$$\mathbf{S} = \frac{1}{\sqrt{m}} \begin{bmatrix} \boldsymbol{\eta}_1^\top \otimes \boldsymbol{\xi}_1^\top \\ \vdots \\ \boldsymbol{\eta}_k^\top \otimes \boldsymbol{\xi}_k^\top \\ \vdots \\ \boldsymbol{\eta}_m^\top \otimes \boldsymbol{\xi}_m^\top \end{bmatrix} \in \mathbb{R}^{m \times n_1 n_2}, \quad (12)$$

where $\boldsymbol{\eta}_k$ and $\boldsymbol{\xi}_k$ are independent copies of $\boldsymbol{\eta} \in \mathbb{R}^{n_1}, \boldsymbol{\xi} \in \mathbb{R}^{n_2}$. The random vectors $\boldsymbol{\eta}$ and $\boldsymbol{\xi}$ are set to be

$$\boldsymbol{\eta} = \frac{1}{\sqrt{q}} \left(\boldsymbol{\phi}^{(1)} \circ \boldsymbol{\sigma}^{(1)} \right) \in \mathbb{R}^{n_1}, \quad \boldsymbol{\xi} = \frac{1}{\sqrt{q}} \left(\boldsymbol{\phi}^{(2)} \circ \boldsymbol{\sigma}^{(2)} \right) \in \mathbb{R}^{n_2}, \quad (13)$$

where $\boldsymbol{\phi}^{(1)} \in \mathbb{R}^{n_1}, \boldsymbol{\phi}^{(2)} \in \mathbb{R}^{n_2}$ are vectors with two sets of i.i.d. zero-mean, unit variance sub-Gaussian variables. We additionally assume the entries of $\boldsymbol{\phi}^{(2)}$ are uniformly bounded. The vectors $\boldsymbol{\sigma}^{(1)}$ and $\boldsymbol{\sigma}^{(2)}$ follow the distributions $\text{Ber}(q)^{n_1}$ and $\text{Ber}(q)^{n_2}$ respectively with $q \in (0, 1]$. We call q as the density level.³

Remark 2.1. The bounded assumption can be imposed on either $\boldsymbol{\phi}^{(1)}$ or $\boldsymbol{\phi}^{(2)}$ due to the symmetry of the sketching construction.

2.2 Main result

In convex analysis, convex cones help represent the optimality condition for the program. The tangent cone of the optimum \mathbf{x}^* with the constraint \mathcal{C} is defined as:

$$\mathcal{K} := \{ \boldsymbol{\Delta} = t(\mathbf{x} - \mathbf{x}^*) \in \mathbb{R}^p, \quad \text{for } t \geq 0 \text{ and } \mathbf{x} \in \mathcal{C} \}. \quad (14)$$

We focus on the transformed cone $\mathbf{A}\mathcal{K} \in \mathbb{R}^{n_1 n_2}$ to measure the gap between $\|\mathbf{A}\hat{\mathbf{x}} - \mathbf{b}\|_2^2$ and $\|\mathbf{A}\mathbf{x}^* - \mathbf{b}\|_2^2$, due to the optimality of \mathbf{x}^* . Of particular interest, our analysis exploits the Gaussian width of the cone $\mathbf{A}\mathcal{K}$ after normalization: $\mathbb{W}(\overline{\mathbf{A}\mathcal{K}})$ defined in (9).

With the necessary preliminaries in place, we now illustrate the main result about the sketching dimension m to guarantee a qualified output for a constrained program.

Theorem 2.1. *Let $n_1, n_2, p, m \in \mathbb{N}^+$. Consider the constrained least squares (1) ($n = n_1 n_2$) with coefficient matrix $\mathbf{A} \in \mathbb{R}^{n_1 n_2 \times p}$, the vector $\mathbf{b} \in \mathbb{R}^{n_1 n_2}$, the optimal solution $\mathbf{x}^* \in \mathbb{R}^p$ and the tangent cone $\mathcal{K} \subset \mathbb{R}^p$ (14). Fix the parameters $q \in (0, 1], \varepsilon \in (0, 1)$ and $\delta \in (0, \frac{1}{2})$. If the sketching matrix $\mathbf{S} \in \mathbb{R}^{m \times n_1 n_2}$ defined in (12)-(13) with density q has the sketching size m satisfying*

$$m \geq C \max \left(\frac{\mathbb{W}(\overline{\mathbf{A}\mathcal{K}})^2}{\varepsilon^2 q^2}, \frac{|\log \delta|}{\varepsilon^2 q} \right), \quad (15)$$

for some finite constant $C > 0$ ⁴, then the sketched solution $\hat{\mathbf{x}} \in \mathbb{R}^p$ of (2) suffices to have

$$\|\mathbf{A}\hat{\mathbf{x}} - \mathbf{b}\|_2^2 \leq (1 + \varepsilon)^2 \|\mathbf{A}\mathbf{x}^* - \mathbf{b}\|_2^2 \quad (16)$$

with probability exceeding $1 - \delta$.

The proof of Theorem 2.1 is in Section 3.2.

We emphasize that the bound of the sketching dimension m (15) is independent of the ambient dimensions n_1 and n_2 . The dependences on $\mathbb{W}(\overline{\mathbf{A}\mathcal{K}})$, the sketching error ε , and failure probability δ are optimal and match the optimal result of the unstructured sub-Gaussian sketches given in [35]. Moreover, the squared Gaussian width $\mathbb{W}(\overline{\mathbf{A}\mathcal{K}})^2$ is proportional to the statistical dimension of

³We note that the density level q is the percentage of nonzeros in expectation for each tensor factor of the sketching matrix \mathbf{S} . As a result, the nonzero percentage of \mathbf{S} is q^2 in expectation.

⁴The constant C in (15) depends on the largest ψ_2 norm of the entries in $\boldsymbol{\phi}^{(1)}, \boldsymbol{\phi}^{(2)}$ and the maximal component magnitude $\max_{k \in [m]} \|\boldsymbol{\xi}_k\|_\infty$, recalling the definitions in (12) - (13). We refer the readers to equation (30) in Section 3.2 for the explicit choice of C .

the cone \mathbf{AK} . The statistical dimension is a robust version of the algebraic dimension for a linear subspace. (See Section 7.6 in [46] for details.) We also see that the sketching dimension bound (15) may change its dependence on the density q , from $\frac{1}{q^2}$ to $\frac{1}{q}$, as q increases. We investigate if such shift of dependence on q exists by the numerical experiment shown in Figure 3.

2.3 Concrete case studies

Theorem 2.1 lays out a unified framework to estimate the sketching dimension via the calculation of the Gaussian width $\mathbb{W}(\overline{\mathbf{AK}})$ based on the data matrix \mathbf{A} and the geometry of the constraint \mathcal{C} . In this subsection, we provide the case studies for different kinds of optimization problems. In each case, we give an explicit computation for $\mathbb{W}(\overline{\mathbf{AK}})$ and hence obtain a guarantee for the sketch \mathbf{S} as a direct corollary from Theorem 2.1.

2.3.1 Unconstrained linear regression

Unconstrained linear regression is the most common example of the convex program (1), by setting \mathcal{C} to be the whole Euclidean space \mathbb{R}^p . The following corollary shows that it suffices to have $\mathcal{O}(\text{rank}(\mathbf{A}))$ rows in the sketching matrix to solve an unconstrained linear regression problem. Our guarantee for the row-wise tensor sub-Gaussian sketch (12) almost matches the optimal result for unstructured sub-Gaussian developed in [35]. We additionally consider a density level q for the sketching design.

Corollary 2.2. *Let $n_1, n_2, p, m \in \mathbb{N}^+$. Consider the linear regression problem (1) with data matrix $\mathbf{A} \in \mathbb{R}^{n_1 n_2 \times p}$ and the constraint $\mathcal{C} = \mathbb{R}^p$. Fix the parameters $q \in (0, 1]$, $\varepsilon \in (0, 1)$ and $\delta \in (0, \frac{1}{2})$. If the sketching matrix $\mathbf{S} \in \mathbb{R}^{m \times n_1 n_2}$ defined in (12)-(13) with density q has the sketching size*

$$m \geq C \max \left(\frac{4 \text{rank}(\mathbf{A})}{\varepsilon^2 q^2}, \frac{|\log \delta|}{\varepsilon^2 q} \right), \tag{17}$$

then the sketched solution $\hat{\mathbf{x}} \in \mathbb{R}^p$ in (2) satisfies the accuracy as in (16) with probability exceeding $1 - \delta$. Above, $C > 0$ is a finite constant.

Proof. The proof of Corollary 2.2 is deduced from (15) in Theorem 2.1 by computing $\mathbb{W}(\overline{\mathbf{AK}})$, which is the Gaussian width of the range of \mathbf{A} intersected with the unit sphere $\mathcal{S}^{n_1 n_2 - 1}$. From Example 3.7 in [45], the Gaussian width of a r -dimensional subset intersected with a unit sphere is upper bounded by $2\sqrt{r}$. Since the dimension of $\text{Range}(\mathbf{A})$ is $\text{rank}(\mathbf{A})$, we have $\mathbb{W}(\text{Range}(\mathbf{A}) \cap \mathcal{S}^{n_1 n_2 - 1}) \leq 2\sqrt{\text{rank}(\mathbf{A})}$. We complete the proof by plugging the above result in (15). \square

2.3.2 Sparse recovery via ℓ_1 -constrained optimization

We study the noiseless sparse recovery problem, which plays a central role in compressive sensing and signal processing. The goal of the recovery is to find a sparse $\hat{\mathbf{x}} \in \mathbb{R}^p$ to approximate an unknown signal $\bar{\mathbf{x}} \in \mathbb{R}^p$ (also sparse in practice), from a small number of random measurements $\Phi \bar{\mathbf{x}} \in \mathbb{R}^m$, with a short wide matrix $\Phi \in \mathbb{R}^{m \times p}$ ($m \ll p$). Furthermore, we can optimize the sparse recovery by an ℓ_1 -constrained least squares problem [18], also known as the Lasso approach [43]. Such optimization has the formulation

$$\hat{\mathbf{x}} = \arg \min_{\|\mathbf{x}\|_1 \leq R} \|\Phi \mathbf{x} - \Phi \bar{\mathbf{x}}\|_2^2, \tag{18}$$

where $R > 0$ is the radius of the ℓ_1 ball.

We show that Theorem 2.1 provides an estimation for the number of measurements m to pursue an accurate recovery from the tensor sub-Gaussian sketching matrix \mathbf{S} (12). Recall the sketched program in (2) and let $n_1 n_2 = p$,

$$\mathbf{S} = \Phi \in \mathbb{R}^{m \times p}, \quad \mathbf{A} = \mathbf{I}_p \in \mathbb{R}^{p \times p}, \quad \mathbf{b} = \bar{\mathbf{x}} \in \mathbb{R}^p, \quad (19)$$

the sketched least squares with an ℓ_1 constraint,

$$\hat{\mathbf{x}} = \arg \min_{\|\mathbf{x}\|_1 \leq R} \|\mathbf{S}\mathbf{A}\mathbf{x} - \mathbf{S}\mathbf{b}\|_2^2 \quad (20)$$

is equivalent to the formulation (18).

Furthermore, in the case of full data acquisition, we denote the one solution

$$\mathbf{x}^* = \arg \min_{\|\mathbf{x}\|_1 \leq R} \|\mathbf{x} - \bar{\mathbf{x}}\|_2^2, \quad (21)$$

to have the least nonzeros among all optimizers.

Corollary 2.3. *Let $m, p \in \mathbb{N}^+$, $\delta \in (0, \frac{1}{2})$, $\varepsilon \in (0, 1)$ and $q \in (0, 1]$. Consider the signal to uncover $\bar{\mathbf{x}} \in \mathbb{R}^p$. Suppose the optimal solution $\mathbf{x}^* \in \mathbb{R}^p$ of (21) has s nonzero entries. If $\Phi \in \mathbb{R}^{m \times p}$ in (18) defined as (12)-(13) ($n_1 n_2 = p$) has the number of measurements*

$$m \geq C \max \left(\frac{\min(36 s \log p, 4p)}{\varepsilon^2 q^2}, \frac{|\log \delta|}{\varepsilon^2 q} \right), \quad (22)$$

then the solution $\hat{\mathbf{x}} \in \mathbb{R}^p$ of (18) satisfies

$$\|\hat{\mathbf{x}} - \bar{\mathbf{x}}\|_2^2 \leq (1 + \varepsilon)^2 \|\mathbf{x}^* - \bar{\mathbf{x}}\|_2^2,$$

with probability exceeding $1 - \delta$. Above, $C > 0$ is a finite constant.

Proof. Due to the equivalence of (18) and (20) via the relationship (19), we apply Theorem 2.1 and obtain a bound of m for successful recovery, by calculating the constrained cone's Gaussian width $\mathbb{W}(\overline{\mathbf{A}}\mathcal{K}) = \mathbb{W}(\overline{\mathcal{K}})$ ($\mathbf{A} = \mathbf{I}_p$). We thus focus on the tangent cone based on the constraint set $\mathcal{C} = \{\mathbf{x} \in \mathbb{R}^p, \|\mathbf{x}\|_1 \leq R\}$. Recalling the definition of \mathcal{K} in (14), due to $\Delta = t(\mathbf{x} - \mathbf{x}^*)$, the cone can be written as

$$\mathcal{K} = \left\{ \Delta \in \mathbb{R}^p \mid \left\| \frac{\Delta}{t} + \mathbf{x}^* \right\|_1 \leq R, \text{ for } t \geq 0 \right\}.$$

1. If the hyperparameter R satisfies $R > \|\bar{\mathbf{x}}\|_1$, then the constrained problem (21) returns \mathbf{x}^* as exactly the true signal $\bar{\mathbf{x}}$, and $\|\mathbf{x}^*\|_1 = \|\bar{\mathbf{x}}\|_1 < R$. The ℓ_1 distance from \mathbf{x}^* to the constraint boundary is strictly positive. Hence for any $\Delta \in \mathbb{R}^p$, there exists $t > 0$ such that $\left\| \frac{\Delta}{t} + \mathbf{x}^* \right\|_1 \leq \left\| \frac{\Delta}{t} \right\|_1 + \|\mathbf{x}^*\|_1 < R$, meaning the tangent cone \mathcal{K} takes over the whole Euclidean space \mathbb{R}^p . Thus $\mathbb{W}(\overline{\mathcal{K}}) = \mathbb{W}(\mathcal{S}^p) \leq 2\sqrt{p}$ is obtained from the proof of Corollary 2.2.
2. If $R \leq \|\bar{\mathbf{x}}\|_1$, since both the constraint set and the least squares problem are strictly convex, the optimal \mathbf{x}^* must be on the boundary of the ℓ_1 ball constraint, implying $\|\mathbf{x}^*\|_1 = R$. Let

the support of \mathbf{x}^* be S and $s = |S|$. We denote Δ_S, Δ_{S^c} the subvectors of Δ in and outside the support S . Note that

$$\begin{aligned} \left\| \frac{\Delta}{t} + \mathbf{x}^* \right\|_1 &= \left\| \left(\frac{\Delta}{t} + \mathbf{x}^* \right)_S \right\|_1 + \left\| \left(\frac{\Delta}{t} + \mathbf{x}^* \right)_{S^c} \right\|_1 \\ &= \left| \left\langle \frac{\Delta_S}{t}, \text{sign}(\mathbf{x}_S^*) \right\rangle + \|\mathbf{x}_S^*\|_1 \right| + \left\| \frac{\Delta_{S^c}}{t} + \mathbf{x}_{S^c}^* \right\|_1 \\ &= \left| \left\langle \frac{\Delta_S}{t}, \text{sign}(\mathbf{x}_S^*) \right\rangle + \|\mathbf{x}^*\|_1 \right| + \left\| \frac{\Delta_{S^c}}{t} \right\|_1 \leq R = \|\mathbf{x}^*\|_1. \end{aligned}$$

This further yields that

$$\left\langle \frac{\Delta_S}{t}, \text{sign}(\mathbf{x}_S^*) \right\rangle + \left\| \frac{\Delta_{S^c}}{t} \right\|_1 = \frac{\langle \Delta_S, \text{sign}(\mathbf{x}_S^*) \rangle + \|\Delta_{S^c}\|_1}{t} \leq 0.$$

Since t is any positive number, the condition can be expressed as

$$\langle \Delta_S, \text{sign}(\mathbf{x}^*) \rangle + \|\Delta_{S^c}\|_1 \leq 0,$$

and

$$\mathcal{K} \subseteq \{ \Delta \in \mathbb{R}^p \mid \langle \text{sign}(\mathbf{x}_S^*), \Delta_S \rangle + \|\Delta_{S^c}\|_1 \leq 0 \}.$$

The Gaussian width computation follows a direct result in the proof of Corollary 3 in [35], that $\mathbb{W}(\overline{\mathcal{K}}) \leq 6\sqrt{s \log p}$.

Combining the discussions of the two cases, we can pick the free parameter R to achieve the smaller $\mathbb{W}(\overline{\mathcal{K}})$ of the two cases and conclude the proof by plugging the bound for $\mathbb{W}(\overline{\mathcal{K}})$: $\min(6\sqrt{s \log p}, 2\sqrt{p})$ in the result (15). \square

3 Bounding the sketching size

In this section, we prove the main result Theorem 2.1 via Theorem 3.1 which provides an estimate of the supreme embedding error over a set from the sketching matrix \mathbf{S} .

3.1 Analysis of tensor sub-Gaussian processes

To bound the error (16) in Theorem 2.1, it is sufficient to bound the embedding errors for the elements in the cone \mathbf{AK} . In this regard, we study the behavior of the (centered) distribution $\mathbf{S}\mathbf{y}$ with the tensor-structured design $\mathbf{S} \in \mathbb{R}^{m \times n_1 n_2}$ (12)-(13) and an arbitrarily chosen vector \mathbf{y} from a set \mathcal{Y} . The analysis provides the knowledge to control the embedding error and the failure probability by adjusting the number of measurements m , and essentially yields the sketching size estimation for convex programs. In particular, we show that the embedding error is bounded by the Gaussian width of the normalized $\overline{\mathcal{Y}}$ (9) over the square root of the sample size m , followed by a Gaussian tail.

Theorem 3.1. *There exist universal constants $c, C_1, C_2 > 0$ for which the following holds. Let $n_1, n_2, m \in \mathbb{N}^+, q \in (0, 1]$ and $\omega \in (0, \frac{1}{2}]$. For any fixed set $\mathcal{Y} \subset \mathbb{R}^{n_1 n_2}$, let the sketching matrix $\mathbf{S} \in \mathbb{R}^{m \times n_1 n_2}$ be defined in (12)-(13) with density q . If the integer $m \geq \frac{C_2 \mathbb{W}(\overline{\mathcal{Y}})^2}{q^2}$, then with probability at least $1 - 4 \exp(-cm \frac{\omega^2 q}{2})$, one can achieve*

$$\sup_{\mathbf{y} \in \overline{\mathcal{Y}}} \left| \|\mathbf{S}\mathbf{y}\|_2^2 - 1 \right| \leq \alpha^2 (\mathcal{M}^2 + 1) \left(\frac{C_1 \mathbb{W}(\overline{\mathcal{Y}})}{\sqrt{m} q} + \omega \right). \quad (23)$$

Here, $\alpha \geq 1^5$ is the maximal ψ_2 norm of entries in $\phi^{(1)}, \phi^{(2)}$ and $\mathcal{M} = \max_{k \in [m]} \|\xi_k\|_\infty$, recalling the definitions in (12)-(13).

The proof of Theorem 3.1 is in Section 4.2.

We stress that the failure probability term $4 \exp(-cm \frac{\omega^2 q}{2})$ is independent of the ambient dimensions n_1, n_2 , which are usually large in practice. The error estimate (23) implies that the density q contributes to reducing the embedding error in a linear decay manner. However, the tensor structure in the sketching design slightly weakens the theoretical result by an extra factor of $\mathcal{M}^2 + 1$ from the maximal coordinate of the tensor factors ξ_k (13). We explore this numerically in Section 5.4 and show that the maximal magnitude in the tensor-structured sketch indeed affects the sketching performance as the theory suggests.

Remark 3.1. The scaling factor $\alpha^2 (\mathcal{M}^2 + 1)$ in the error bound (23) is a finite constant. In fact, recalling (13), the entries of $\xi_k \in \mathbb{R}^{n_2}$ are products of bounded random variables and Bernoulli variables, so they can be uniformly bounded by a finite \mathcal{M} . Furthermore, the entries of $\phi^{(1)}, \phi^{(2)}$ are sub-Gaussian variables, thus the ψ_2 norms can also be uniformly bounded by a finite number α .

3.2 Proof of Theorem 2.1

Proof. The proof follows the ideas of Lemma 1, 2, 3 in [35]. The next lemma relates the sketching error (16) with two specific terms D_1 and D_2 , both of which can be further bounded by the supreme embedding error in (23) over the cone \mathbf{AK} .

Lemma 3.2. *(Lemma 1 in [35].) Let $n_1, n_2, p, m \in \mathbb{N}^+$. Consider the least squares (1) with data matrix $\mathbf{A} \in \mathbb{R}^{n_1 n_2 \times p}$, the vector $\mathbf{b} \in \mathbb{R}^{n_1 n_2}$, the optimal solution $\mathbf{x}^* \in \mathbb{R}^p$ and the tangent cone $\mathcal{K} \subset \mathbb{R}^p$ defined in (14). For any fixed matrix $\mathbf{S} \in \mathbb{R}^{m \times n_1 n_2}$, define the two quantities*

$$D_1 = \inf_{\mathbf{y} \in \mathbf{AK}} \|\mathbf{S}\mathbf{y}\|_2^2, \quad D_2 = \sup_{\mathbf{y} \in \mathbf{AK}} \left| \left\langle \frac{\mathbf{A}\mathbf{x}^* - \mathbf{b}}{\|\mathbf{A}\mathbf{x}^* - \mathbf{b}\|_2}, (\mathbf{S}^\top \mathbf{S} - \mathbf{I}_{n_1 n_2}) \mathbf{y} \right\rangle \right|.$$

Then the sketched solution $\hat{\mathbf{x}}$ of (2) satisfies

$$\|\mathbf{A}\hat{\mathbf{x}} - \mathbf{b}\|_2^2 \leq \left(1 + \frac{2D_2}{D_1} \right) \|\mathbf{A}\mathbf{x}^* - \mathbf{b}\|_2^2. \quad (24)$$

⁵The value of α is greater than 1 is because $\phi^{(1)}, \phi^{(2)}$ both have entries with zero-mean and standard deviation of 1. And the standard deviation of a zero-mean r.v., which is essentially the ℓ_2 norm, is no more than its ψ_2 norm. We refer the readers to Example 2.7.12 and 2.7.13 in [46] for details.

Remark 3.2. We note that there is a difference between the set-ups of Lemma 3.2 and Lemma 1 in [35]. Lemma 3.2 considers the vector \mathbf{y} on the normalized set $\overline{\mathbf{AK}}$ while [35] defines \mathbf{y} to be on the intersection of \mathbf{AK} and the unit sphere. In fact, it can be shown that $\overline{\mathbf{AK}} = \mathbf{AK} \cap \mathcal{S}^{n_1 n_2 - 1}$, hence the result of [35] is applicable for Lemma 3.2. We refer the readers to the proof of Lemma 1 in [35] for details.

It remains to bound D_1, D_2 to keep the accuracy of $\hat{\mathbf{x}}$ for Theorem 2.1. Respectively applying Theorem 3.1, we obtain a lower bound for D_1 and an upper bound for D_2 .

Lemma 3.3. *There exist universal constants $c, C_1, C_2 > 0$ for which the following holds. Follow the same setting in Lemma 3.2. Fix $q \in (0, 1], \omega \in (0, \frac{1}{2}]$ and the integer $m \geq \frac{C_2 \mathbb{W}(\overline{\mathbf{AK}})^2}{q^2}$, then for a sketching matrix $\mathbf{S} \in \mathbb{R}^{m \times n_1 n_2}$ defined in (12)-(13) and $\theta = \alpha^2 (\mathcal{M}^2 + 1)$ given in (23),*

1. *the event*

$$D_1 = \inf_{\mathbf{y} \in \overline{\mathbf{AK}}} \|\mathbf{S}\mathbf{y}\|_2^2 \geq 1 - \theta \left(\frac{C_1 \mathbb{W}(\overline{\mathbf{AK}})}{\sqrt{m}q} + \omega \right) \quad (25)$$

achieves with probability exceeding $1 - 4 \exp(-cm \frac{\omega^2 q}{2})$;

2. *another event*

$$D_2 = \sup_{\mathbf{y} \in \overline{\mathbf{AK}}} \left| \left\langle \frac{\mathbf{Ax}^* - \mathbf{b}}{\|\mathbf{Ax}^* - \mathbf{b}\|_2}, (\mathbf{S}^\top \mathbf{S} - \mathbf{I}_{n_1 n_2}) \mathbf{y} \right\rangle \right| \leq \theta \left(\frac{5 C_1 \mathbb{W}(\overline{\mathbf{AK}})}{\sqrt{m}q} + 3\omega \right) \quad (26)$$

achieves with probability exceeding $1 - 24 \exp(-cm \frac{\omega^2 q}{2})$.

We show the proof of Lemma 3.3 in Appendix A.

We now prove Theorem 2.1. For fixed $\varepsilon \in (0, 1)$ and $\delta \in (0, \frac{1}{2})$ given in Theorem 2.1, we let

$$\omega = \frac{\varepsilon}{16\theta + 2\theta\varepsilon} < \frac{\varepsilon}{16\theta} < \frac{1}{2}, \quad (27)$$

where $\theta = \alpha^2 (\mathcal{M}^2 + 1) \geq 1$ is set in Lemma 3.3. Suppose $m \geq \frac{C_2 \mathbb{W}(\overline{\mathbf{AK}})^2}{q^2}$, we are eligible to apply Lemma 3.3. By plugging in the bounds of D_1, D_2 provided in (25), (26) and summing up the failure probabilities, then together with (24) in Lemma 3.2, we have the accuracy estimation:

$$\|\mathbf{A}\hat{\mathbf{x}} - \mathbf{b}\|_2^2 \leq \left(1 + \frac{\theta \left(\frac{10 C_1 \mathbb{W}(\overline{\mathbf{AK}})}{\sqrt{m}q} + 6\omega \right)}{1 - \theta \left(\frac{C_1 \mathbb{W}(\overline{\mathbf{AK}})}{\sqrt{m}q} + \omega \right)} \right)^2 \|\mathbf{Ax}^* - \mathbf{b}\|_2^2 \quad (28)$$

achieves with probability $1 - 28 \exp(-cm \frac{\omega^2 q}{2})$.

Furthermore, we assume

$$m \geq \max \left(\frac{C_1^2 \mathbb{W}(\overline{\mathbf{AK}})^2}{\omega^2 q^2}, \frac{12 |\log \delta|}{c \omega^2 q}, \frac{C_2 \mathbb{W}(\overline{\mathbf{AK}})^2}{q^2} \right), \quad (29)$$

then $\frac{C_1 \mathbb{W}(\overline{\mathbf{AK}})}{\sqrt{m}q} \leq \omega$. By (28), one can achieve

$$\begin{aligned} \|\mathbf{A}\hat{\mathbf{x}} - \mathbf{b}\|_2^2 &\leq \left(1 + \frac{16\theta\omega}{1 - 2\theta\omega} \right)^2 \|\mathbf{Ax}^* - \mathbf{b}\|_2^2 \\ &= (1 + \varepsilon)^2 \|\mathbf{Ax}^* - \mathbf{b}\|_2^2, \end{aligned}$$

with probability exceeding $1 - \delta$. The relationship $\varepsilon = \frac{16\theta\omega}{1-2\theta\omega}$ is derived from (27). The failure probability $\delta > 28 \exp(-cm \frac{\omega^2 q}{2})$ is due to $\delta \in (0, \frac{1}{2})$ and

$$m \geq \frac{12 |\log \delta|}{c\omega^2 q} > \frac{2 |\log \frac{\delta}{28}|}{c\omega^2 q}.$$

From the choice of m in (29) and the relation of ε and ω in (27), we define a finite constant

$$C = \max \left(16^2 \theta^2 C_1^2, \frac{16^2 \cdot 12 \theta^2}{c}, C_2 \right), \quad (30)$$

where $\theta = \alpha^2 (\mathcal{M}^2 + 1)$ given in (23) is a finite constant, see Remark 3.1, and only depends on the distribution of the sketching matrix \mathbf{S} . Then the assumption (29) on m can be simplified via (27) as follows

$$\begin{aligned} m &\geq C \max \left(\frac{\mathbb{W}(\overline{\mathbf{A}\mathcal{K}})^2}{\varepsilon^2 q^2}, \frac{|\log \delta|}{\varepsilon^2 q} \right) \\ &\geq \max \left(\frac{16^2 \theta^2 C_1^2 \mathbb{W}(\overline{\mathbf{A}\mathcal{K}})^2}{\varepsilon^2 q^2}, \frac{16^2 \theta^2 12 |\log \delta|}{c \varepsilon^2 q}, \frac{C_2 \mathbb{W}(\overline{\mathbf{A}\mathcal{K}})^2}{\varepsilon^2 q^2} \right) \\ &\geq \max \left(\frac{C_1^2 \mathbb{W}(\overline{\mathbf{A}\mathcal{K}})^2}{\omega^2 q^2}, \frac{12 |\log \delta|}{c \omega^2 q}, \frac{C_2 \mathbb{W}(\overline{\mathbf{A}\mathcal{K}})^2}{q^2} \right). \end{aligned}$$

This ensures the sketched solution $\hat{\mathbf{x}}$ achieves (16) with probability exceeding $1 - \delta$ and concludes our proof. \square

4 Bounding the error with Gaussian width

In this section, we give the proof of Theorem 3.1 and validate that the Gaussian width is the correct measure to bound the tensorized sub-Gaussian processes approximation error. The major tool is the standard generic chaining approach [41].

4.1 Proof ingredients

We first present the crucial supporting proposition and lemmas for Theorem 3.1. These results and their proofs are incorporated in Appendices B to E.

The cornerstone of Theorem 3.1 is the sparse Hanson-Wright inequality in Theorem 1.1 of [47] for a single sub-Gaussian process. We present an extension of the result by averaging the quadratic forms from multiple independent processes. The following lemma shows how the density level q affects the sub-Gaussian tail of the quadratic form.

Proposition 4.1. *There exists a universal constant $c > 0$ for which the following holds. Let $n, m \in \mathbb{N}^+$ and $q \in (0, 1]$. For any determined squared matrices $\mathbf{A}_k \in \mathbb{R}^{n \times n}$ for $k \in [m]$, draw m independent copies \mathbf{s}_k of $\mathbf{s} = \boldsymbol{\phi} \circ \boldsymbol{\sigma} \in \mathbb{R}^n$, where $\boldsymbol{\phi} \in \mathbb{R}^n$ has independent zero-mean entries with bounded ψ_2 norms, and the vector $\boldsymbol{\sigma} \sim \text{Ber}(q)^n$. Then for every $t > 0$,*

$$\Pr \left(\left| \frac{1}{m} \sum_{k=1}^m \mathbf{s}_k^\top \mathbf{A}_k \mathbf{s}_k - \mathbb{E} \mathbf{s}_k^\top \mathbf{A}_k \mathbf{s}_k \right| > t \right) \leq 2 \exp \left(-cm \min \left(\frac{t}{K_1 \beta^2}, \frac{t^2}{K_2^2 \beta^4 q} \right) \right), \quad (31)$$

where $\beta > 0$ is the maximal ψ_2 norm of entries in $\boldsymbol{\phi}$, $K_1 = \max_{k \in [m]} \|\mathbf{A}_k\|_2$ and $K_2 = \max_{k \in [m]} \|\mathbf{A}_k\|_F$.

Without the loss of generality, we assume the fixed set $\mathbf{y} = \bar{\mathbf{y}}$ is on the unit sphere $\mathcal{S}^{n_1 n_2 - 1}$ below and in the proof of Theorem 3.1 (Section 4.2). For any vector $\mathbf{y} \in \mathcal{Y}$, recalling the sketching matrix \mathbf{S} defined in (12)-(13), we focus on two related random variables

$$H(\mathbf{y}) = \left(\frac{1}{m} \sum_{k=1}^m \langle \boldsymbol{\eta}_k \otimes \boldsymbol{\xi}_k, \mathbf{y} \rangle^2 \right)^{1/2} = \|\mathbf{S}\mathbf{y}\|_2, \quad (32)$$

$$Q(\mathbf{y}) = \frac{1}{m} \sum_{k=1}^m \langle \boldsymbol{\eta}_k \otimes \boldsymbol{\xi}_k, \mathbf{y} \rangle^2 - \|\mathbf{y}\|_2^2 = \|\mathbf{S}\mathbf{y}\|_2^2 - \|\mathbf{y}\|_2^2.$$

We then introduce the basic estimates of H, Q by applying Proposition 4.1. The concentration results will be used in the chaining procedure.

Lemma 4.2. *There exists a universal constant $c > 0$ for which the following holds. Let $n_1, n_2, m \in \mathbb{N}^+$ and $q \in (0, 1]$. For every $\mathbf{y}, \mathbf{y}' \in \mathcal{Y} \subset \mathcal{S}^{n_1 n_2 - 1} (\mathbf{y} \neq \mathbf{y}')$, consider H, Q defined in (32) with $\alpha \geq 1$ and $\mathcal{M} \geq 0$ given in Theorem 3.1.*

1. For every $u > 0$,

$$\Pr(|Q(\mathbf{y})| \geq u \alpha^2 (\mathcal{M}^2 + 1)) \leq 4 \exp(-c m \min(u q, u^2 q)); \quad (33)$$

2. for every $u > 0$,

$$\Pr(|Q(\mathbf{y}) - Q(\mathbf{y}')| \geq u \alpha^2 (\mathcal{M}^2 + 1) \|\mathbf{y} - \mathbf{y}'\|_2) \leq 4 \exp\left(-c m \min\left(\frac{u q}{\sqrt{2}}, \frac{u^2 q}{2}\right)\right); \quad (34)$$

3. for $u \geq \sqrt{1 + \frac{1}{\alpha^2}}$,

$$\Pr\left(H(\mathbf{y} - \mathbf{y}') \geq u \alpha \sqrt{\mathcal{M}^2 + 1} \|\mathbf{y} - \mathbf{y}'\|_2\right) \leq 4 \exp\left(-c m \frac{u^2 q}{1 + \frac{1}{\alpha^2}}\right). \quad (35)$$

We apply the generic chaining technique [41] and follow the detailed illustrations in [28]. Lemma 4.3 proves that one can project the whole set \mathcal{Y} to a subset \mathcal{Y}' of restricted cardinality and maintain a small projection error with high probability. The result depends on a fine construction of a subset \mathcal{Y}' . Lemma 4.4 bounds the supremum embedding error by \mathbf{S} over such subset.

Lemma 4.3. *There exists a universal constant $C' > 0$ for which the following holds. Follow the same set-up in Lemma 4.2. There is a subset $\mathcal{Y}' \subset \mathcal{Y} \subset \mathcal{S}^{n_1 n_2 - 1}$ such that $|\mathcal{Y}'| \leq 4^m$ and with probability at least $1 - \exp(-4m)$, we have*

$$\sup_{\mathbf{y} \in \mathcal{Y}} H(\mathbf{y} - \pi(\mathbf{y})) \leq C' \alpha \sqrt{\mathcal{M}^2 + 1} \frac{\mathbb{W}(\mathcal{Y})}{\sqrt{m q}}, \quad (36)$$

where $\pi(\mathbf{y})$ is a nearest point to \mathbf{y} in \mathcal{Y}' under $\|\cdot\|_2$ metric.

Lemma 4.4. *There exists a universal constant $C'' > 0$ for which the following holds. Follow the same set-up in Lemma 4.2. Fix any subset $\mathcal{Y}' \subset \mathcal{Y} \subset \mathcal{S}^{n_1 n_2 - 1}$ such that $|\mathcal{Y}'| \leq 4^m$. Then for every $0 < \omega < 1$,*

$$\sup_{\mathbf{y} \in \mathcal{Y}'} |Q(\mathbf{y})| \leq \alpha^2 (\mathcal{M}^2 + 1) \left(C'' \frac{W(\mathcal{Y})}{\sqrt{m} q} + \omega \right) \quad (37)$$

holds with probability at least $1 - 3 \exp\left(-c m \frac{\omega^2 q}{2}\right)$.

4.2 Proof of Theorem 3.1

Proof. Without the loss of generality, we assume $\mathcal{Y} = \overline{\mathcal{Y}}$ is on the unit sphere $\mathcal{S}^{n_1 n_2 - 1}$. Let \mathcal{Y}' be one subset of \mathcal{Y} that satisfies the condition stated in Lemma 4.3. We denote a projection by $\pi : \mathcal{Y} \rightarrow \mathcal{Y}'$, which maps the points in \mathcal{Y} to their nearest points in \mathcal{Y}' respectively.

The goal of Theorem 3.1 is to estimate $\sup_{\mathbf{y} \in \mathcal{Y}} \left| \|\mathbf{S}\mathbf{y}\|_2^2 - \|\mathbf{y}\|_2^2 \right| = \sup_{\mathbf{y} \in \mathcal{Y}} |Q(\mathbf{y})|$. Notice that $Q(\mathbf{y})$ and $H(\mathbf{y})$ defined in (32), we rewrite $Q(\mathbf{y})$ in the following form:

$$\begin{aligned} Q(\mathbf{y}) &= Q(\pi(\mathbf{y})) + Q(\mathbf{y} - \pi(\mathbf{y})) + 2\langle \mathbf{S}(\mathbf{y} - \pi(\mathbf{y})), \mathbf{S}\pi(\mathbf{y}) \rangle - 2\langle \mathbf{y} - \pi(\mathbf{y}), \pi(\mathbf{y}) \rangle \\ &= Q(\pi(\mathbf{y})) + H(\mathbf{y} - \pi(\mathbf{y}))^2 - \|\mathbf{y} - \pi(\mathbf{y})\|_2^2 + 2\langle \mathbf{S}(\mathbf{y} - \pi(\mathbf{y})), \mathbf{S}\pi(\mathbf{y}) \rangle - 2\langle \mathbf{y} - \pi(\mathbf{y}), \pi(\mathbf{y}) \rangle \\ &= Q(\pi(\mathbf{y})) + H(\mathbf{y} - \pi(\mathbf{y}))^2 + 2\langle \mathbf{S}(\mathbf{y} - \pi(\mathbf{y})), \mathbf{S}\pi(\mathbf{y}) \rangle - \|\mathbf{y} - \pi(\mathbf{y})\|_2^2 - 2\langle \mathbf{y} - \pi(\mathbf{y}), \pi(\mathbf{y}) \rangle \end{aligned} \quad (38)$$

Since both $\mathbf{y}, \pi(\mathbf{y})$ are on the unit sphere,

$$-\|\mathbf{y} - \pi(\mathbf{y})\|_2^2 - 2\langle \mathbf{y} - \pi(\mathbf{y}), \pi(\mathbf{y}) \rangle = -(\|\mathbf{y}\|_2^2 - \|\pi(\mathbf{y})\|_2^2) = 0,$$

continue from (38),

$$Q(\mathbf{y}) = Q(\pi(\mathbf{y})) + H(\mathbf{y} - \pi(\mathbf{y}))^2 + 2\langle \mathbf{S}(\mathbf{y} - \pi(\mathbf{y})), \mathbf{S}\pi(\mathbf{y}) \rangle.$$

We then apply triangles inequality and Hölder's inequality to derive the following,

$$|Q(\mathbf{y})| \leq |Q(\pi(\mathbf{y}))| + H(\mathbf{y} - \pi(\mathbf{y}))^2 + 2H(\mathbf{y} - \pi(\mathbf{y}))H(\pi(\mathbf{y})).$$

Taking supremum over \mathcal{Y} for both sides above and notice that $\pi(\mathbf{y}) \in \mathcal{Y}'$, we have

$$\sup_{\mathbf{y} \in \mathcal{Y}} |Q(\mathbf{y})| \leq \sup_{\mathbf{y}' \in \mathcal{Y}'} |Q(\mathbf{y}')| + \sup_{\mathbf{y} \in \mathcal{Y}} H(\mathbf{y} - \pi(\mathbf{y}))^2 + 2 \left(\sup_{\mathbf{y} \in \mathcal{Y}} H(\mathbf{y} - \pi(\mathbf{y})) \right) \left(\sup_{\mathbf{y}' \in \mathcal{Y}'} H(\mathbf{y}') \right). \quad (39)$$

The inequality (39) indicates that $\sup_{\mathbf{y} \in \mathcal{Y}} |Q(\mathbf{y})|$ is bounded by three components. In the following, we handle the first term $\sup_{\mathbf{y}' \in \mathcal{Y}'} |Q(\mathbf{y}')|$ by Lemma 4.4 and the second by Lemma 4.3. The third term is controlled simultaneously since each factor can be bounded from the first and second components respectively.

1. Fix $\omega \in (0, \frac{1}{2}]$ stated in Theorem 3.1, since $|\mathcal{Y}'| \leq 4^m$, we apply Lemma 4.4. Then with probability at least $1 - 3 \exp\left(-c m \frac{\omega^2 q}{2}\right)$, one has

$$\sup_{\mathbf{y}' \in \mathcal{Y}'} |Q(\mathbf{y}')| \leq \alpha^2 (\mathcal{M}^2 + 1) \left(C'' \frac{W(\mathcal{Y})}{\sqrt{m} q} + \omega \right). \quad (40)$$

Moreover, if we assume the integer $m \geq \frac{4C''^2 \mathbb{W}(\mathcal{Y})^2}{q^2}$, then

$$C'' \frac{\mathbb{W}(\mathcal{Y})}{\sqrt{m}q} + \omega \leq 1.$$

This further implies that

$$\sup_{\mathbf{y}' \in \mathcal{Y}'} H(\mathbf{y}')^2 \leq \sup_{\mathbf{y}' \in \mathcal{Y}'} |Q(\mathbf{y}')| + \|\mathbf{y}'\|_2^2 \leq \alpha^2 (\mathcal{M}^2 + 1) + 1 \leq 2\alpha^2 (\mathcal{M}^2 + 1).$$

where we use (40) and $\|\mathbf{y}'\|_2 = 1$ in the second inequality above. The last inequality holds because $\alpha \geq 1$ ⁵. Consequently,

$$\sup_{\mathbf{y}' \in \mathcal{Y}'} H(\mathbf{y}') \leq \sqrt{2} \alpha \sqrt{\mathcal{M}^2 + 1}. \quad (41)$$

2. To deal with the second term in (39), since we define the subset \mathcal{Y}' to satisfy the condition in Lemma 4.3, we apply Lemma 4.3,

$$\sup_{\mathbf{y} \in \mathcal{Y}} H(\mathbf{y} - \pi(\mathbf{y})) \leq \alpha \sqrt{\mathcal{M}^2 + 1} C' \frac{\mathbb{W}(\mathcal{Y})}{\sqrt{m}q}, \quad (42)$$

or equivalently,

$$\sup_{\mathbf{y} \in \mathcal{Y}} H(\mathbf{y} - \pi(\mathbf{y}))^2 \leq \alpha^2 (\mathcal{M}^2 + 1) \left(C' \frac{\mathbb{W}(\mathcal{Y})}{\sqrt{m}q} \right)^2, \quad (43)$$

achieves with probability at least $1 - \exp(-4m)$.

We further assume that $m \geq \frac{C'^2 \mathbb{W}(\mathcal{Y})^2}{q}$, then $C' \frac{\mathbb{W}(\mathcal{Y})}{\sqrt{m}q} \leq 1$. And (43) implies that

$$\sup_{\mathbf{y} \in \mathcal{Y}} H(\mathbf{y} - \pi(\mathbf{y}))^2 \leq \alpha^2 (\mathcal{M}^2 + 1) C' \frac{\mathbb{W}(\mathcal{Y})}{\sqrt{m}q}. \quad (44)$$

We now plug all the bounds in (40), (44), (42) and (41) into the partition form in (39). Consequently, the following event

$$\sup_{\mathbf{y} \in \mathcal{Y}} |Q(\mathbf{y})| \leq \alpha^2 (\mathcal{M}^2 + 1) \left[(\sqrt{q} C' + \sqrt{2q} C' + C'') \frac{\mathbb{W}(\mathcal{Y})}{\sqrt{m}q} + \omega \right] \quad (45)$$

holds with failure probability no more than $\exp(-4m) + 3\exp(-cm \frac{\omega^2 q}{2})$.

Notice that $q \in (0, 1]$ and the constant $c \leq \frac{1}{4e}$ as shown in [47], it follows that $0 < \omega \leq \frac{1}{2} \leq \sqrt{\frac{8}{cq}}$. This further implies that $\exp(-4m) \leq \exp(-cm \frac{\omega^2 q}{2})$, so the failure probability can be upper bounded by $4\exp(-cm \frac{\omega^2 q}{2})$.

To conclude, given the assumption

$$m \geq \frac{C_2 \mathbb{W}(\mathcal{Y})^2}{q^2} \geq \max\left(\frac{C'^2}{q}, \frac{4C''^2}{q^2}\right) \mathbb{W}(\mathcal{Y})^2,$$

then from (45),

$$\sup_{\mathbf{y} \in \mathcal{Y}} \left| \|\mathbf{S}\mathbf{y}\|_2^2 - \|\mathbf{y}\|_2^2 \right| = \sup_{\mathbf{y} \in \mathcal{Y}} |Q(\mathbf{y})| \leq \alpha^2 (\mathcal{M}^2 + 1) \left(C_1 \frac{W(\mathcal{Y})}{\sqrt{mq}} + \omega \right)$$

holds with probability no less than $1 - 4 \exp(-cm \frac{\omega^2 q}{2})$, where the universal constants C_1, C_2 are set to satisfy

$$\begin{cases} C_1 \geq \sqrt{q} C' + \sqrt{2q} C' + C'', \\ C_2 \geq \max(C''^2 q, 4 C''^2). \end{cases}$$

The proof of Theorem 3.1 is complete. \square

5 Numerical experiments

In this section, we demonstrate the numerical performance for the row-wise tensor sketching matrix $\mathbf{S} \in \mathbb{R}^{m \times n_1 n_2}$ defined in (12)-(13). Specifically, we choose a common case of \mathbf{S} to be: Gaussian+Rademacher (G+R), meaning the tensor component $\phi^{(1)} \in \mathbb{R}^{n_1}$ in (13) follows the standard normal distribution $\mathcal{N}(\mathbf{0}, \mathbf{I}_{n_1})$, while the other $\phi^{(2)} \in \{-1, 1\}^{n_2}$ is a Rademacher vector whose entries are i.i.d. and take the values 1 and -1 with equal probability $1/2$.

We implement the sketch \mathbf{S} on the unconstrained linear regression

$$\mathbf{x}^* = \arg \min_{\mathbf{x} \in \mathbb{R}^p} \|\mathbf{A}\mathbf{x} - \mathbf{b}\|_2^2. \quad (46)$$

We focus on three types of linear regressions where the data matrix $\mathbf{A} \in \mathbb{R}^{n_1 n_2 \times p}$ has different properties:

1. **Well-conditioned program.**

In this setting, the data matrix \mathbf{A} has a relatively small condition number.

2. **Ill-conditioned program.**

For the ill-conditioned problem, we build the condition number of \mathbf{A} to be large, for instance, 10^4 .

3. **Structured program.**

As we mentioned in Section 2.1, in the structured program, the columns of the matrix \mathbf{A} admit tensor structure:

$$\mathbf{a}_j = \mathbf{f}_j \otimes \mathbf{g}_j, \quad \text{for } j \in [p]. \quad (47)$$

In terms of building the input system, we generate the matrix \mathbf{A} based on the singular value decomposition:

$$\mathbf{A}_{n_1 n_2 \times p} = \mathbf{U}_{n_1 n_2 \times p} \mathbf{\Sigma}_{p \times p} \mathbf{V}_{p \times p}^\top,$$

where the left and right factors \mathbf{U}, \mathbf{V} are built from the orthogonal matrices \mathbf{Q} in QR decompositions of standard Gaussian matrices, whose entries are i.i.d. and normally distributed with zero mean and unit variance. For a well-conditioned matrix \mathbf{A} with a small condition number,

the singular values are drawn from normal distribution $\mathcal{N}(1, 0.04)$ and thus are centered around 1 with high probability. For a ill-conditioned matrix \mathbf{A} , we set the singular values to be

$$\Sigma_{j,j} = 10^{(-4) \frac{j-1}{p-1}}, \quad \text{for } j \in [p].$$

The condition number of \mathbf{A} is thus $\Sigma_{1,1}/\Sigma_{p,p} = 10^4$. For a structured matrix \mathbf{A} , we instead form two factor matrices $\mathbf{F} = [\mathbf{f}_1, \dots, \mathbf{f}_p] \in \mathbb{R}^{n_1 \times p}$ and $\mathbf{G} = [\mathbf{g}_1, \dots, \mathbf{g}_p] \in \mathbb{R}^{n_2 \times p}$ respectively, following the way of generating a well-conditioned matrix and then construct \mathbf{A} by the rule (47). To form the input vector $\mathbf{b} \in \mathbb{R}^{n_1 n_2}$, first we generate a reference vector $\mathbf{x}_{\text{ref}} \in \mathbb{R}^p$ following the distribution $\mathcal{N}(\mathbf{1}, 0.25 \mathbf{I}_p)$ and a small noise vector following $\mathcal{N}(\mathbf{0}, 10^{-2} \mathbf{I}_{n_1 n_2})$. We build the data vector \mathbf{b} as

$$\mathbf{b} = \mathbf{A} \mathbf{x}_{\text{ref}} + \text{noise}.$$

In the numerical experiments, we perform the sketching construction \mathbf{S} on the aforementioned three types of linear regressions. We then compare the performance of \mathbf{S} with that of the standard Gaussian matrix. We denote $\mathbf{x}^* \in \mathbb{R}^p$ as (46), and $\hat{\mathbf{x}} \in \mathbb{R}^p$ the sketched solution $\hat{\mathbf{x}} = \arg \min_{\mathbf{x} \in \mathbb{R}^p} \|\mathbf{S} \mathbf{A} \mathbf{x} - \mathbf{S} \mathbf{b}\|_2^2$. To measure the quality of a sketched solution $\hat{\mathbf{x}}$, we define

$$\text{error ratio} = \left| \frac{\|\mathbf{A} \hat{\mathbf{x}} - \mathbf{b}\|_2^2 - \|\mathbf{A} \mathbf{x}^* - \mathbf{b}\|_2^2}{\|\mathbf{A} \mathbf{x}^* - \mathbf{b}\|_2^2} \right| \quad (48)$$

For all numerical tests below, we calculate the error ratio as the average of 100 independent simulations.

Notice that (16) in Theorem 2.1 implies that the above error ratio is bounded by $\varepsilon^2 + 2\varepsilon$ with the parameter ε used in the theoretical results, indicating that

$$\text{error ratio} = \begin{cases} O(\varepsilon), & \varepsilon \text{ and error ratio are relatively small,} \\ O(\varepsilon^2), & \varepsilon \text{ and error ratio are relatively large.} \end{cases} \quad (49)$$

In figures 1 to 3, we plot the error ratios respectively depending on different choices of the parameters:

1. **the sketching dimension m ,**
2. **the number of unknown variables p ,**
3. **the density level q .**

The plots are all in the log-log form.

5.1 Dependence on the sketching size m

It is of interest to test how the sketching dimension m affects the quality of our sketching matrix \mathbf{S} . Figure 1 presents the empirical performance of \mathbf{S} as the sketching dimension m varies. We summarize the numerical observations as follows:

1. In the small error regime (under the scale between 10^0 and 10^{-1}), the roughly parallel lines validate the theory that the G+R sketch has the same performance as that of the standard Gaussian sketch.

2. In contrast, there are rapid drops in the large error ratio regime for the G+R sketching in both well and ill-conditioned programs. Such phenomena can be explained by the quantitative shift of the dependence on ε shown in (49). More specifically, the error ratio decays at the order $\mathcal{O}(\varepsilon^2)$ when the sketching size m is small but gradually drops at a slower rate $\mathcal{O}(\varepsilon)$ as m grows.
3. Unlike its performance in the unstructured programs, the G+R sketching does not have a drastic decay in the structured program. This may suggest a better estimate of the sketching dimension for tensor-structured programs.

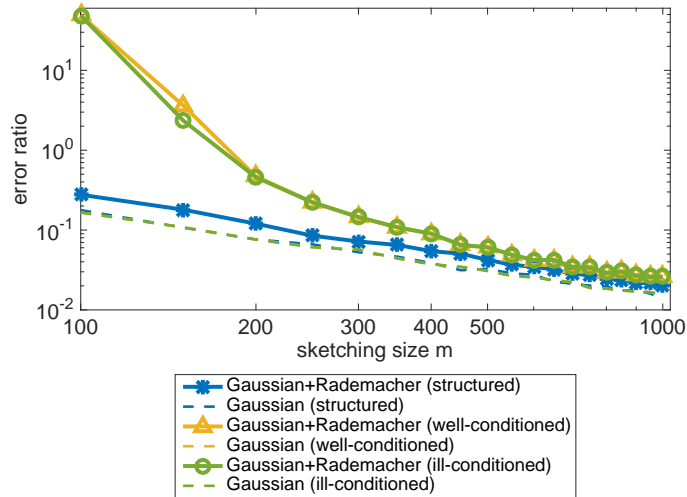


Figure 1: We plot in solid curves the error ratios averaged over 100 trials of the G+R sketching with density $q = 0.2$, respectively on the well-conditioned, ill-conditioned and structured linear regressions with varying sketching size m . In comparison, the performance of unstructured Gaussian sketching matrix is plotted in dash lines on the same three types of regression problems for reference. The size of the regression problems is set as $n_1 n_2 = 64^2$ by $p = 15$.

5.2 Dependence on the number of unknowns p

The matrix $\mathbf{A} \in \mathbb{R}^{n_1 n_2 \times p}$ is full rank with high probability due to our construction method, thus the number of unknowns $p = \text{rank}(\mathbf{A})$ considering $n_1, n_2 \geq p$. We show in Figure 2 the performance of the sketching strategy as the number of unknowns p changes.

1. When the error ratios are relatively small, i.e. under the scale 10^{-1} , the G+R construction for all three types of programs is shown to have the same dependence as the standard Gaussian matrix on p , or equivalently $\text{rank}(\mathbf{A})$, given that the slopes are rather similar. This observation is important and provides numerical support for our main results Theorem 2.1 and Corollary 2.2, that the tensor-structured sketching maintains the same optimal dependence on $\text{rank}(\mathbf{A})$ as conventional Gaussian matrix in unconstrained linear regressions.
2. There are rises in the later part of the solid curves for well and ill-conditioned programs when the errors are getting bigger. The reason is still the quantitative change of the error ratio, see (49).

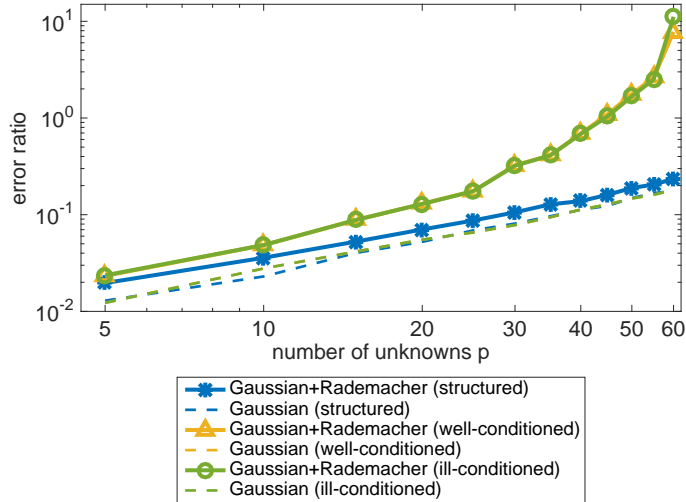


Figure 2: We plot the sketching error ratios with varying number of unknown variables p with fixed ambient dimension $n_1 n_2 = 64^2$ for three different types of linear regression programs. We fix the sketching dimension $m = 400$. We compare the performances of the G+R sketching constructed with density $q = 0.2$ and standard Gaussian sketching.

5.3 Dependence on the density level q

Figure 3 clearly shows that the sketching accuracy improves when the density level q in the construction of \mathbf{S} increases.

1. Again, abrupt drops appear in the beginning of the plots, which can be explained by the quantitative change in the error ratio, see (49). In the later part of the plots for well and ill-conditioned programs, i.e. $q \in [0.2, 0.75]$, the two solid curves overlap and smoothly decay at the same rate. Such decay is supported by the second term in our theoretical bound (15) when q is relatively large, implying that $\varepsilon \sim \frac{1}{\sqrt{q}}$ if m is fixed. In fact, a linear fitting calculation suggests that the two solid curves decay at the slope -0.62 , which roughly agrees with the theoretical prediction slope -0.5 .
2. When the density level is greater than 0.4, the performances of the G+R sketchings are nearly the same on all three different regression problems. Moreover, the plots suggest that for density level $q \geq 0.6$, a sparse tensor sketching strategy may achieve the same performance of unstructured dense Gaussians.

5.4 Bounded vs unbounded sketches

The theoretical result (23) in Theorem 3.1 indicates that the embedding error contains a factor $(\mathcal{M}^2 + 1)$, which depends on the maximal magnitude in one tensor component of the sketch. This is a consequence of our assumption in the sketching matrix (12)-(13) that one of the tensor factors is uniformly bounded. In Figure 4, we investigate if the bounded condition has an impact on the sketching performance. In the experiment set-up, besides for the G+R construction, we also use the Gaussian+Gaussian (G+G) and Rademacher+Rademacher (R+R) as the examples for unbounded and bounded sketches. They both fit into the row-wise tensor sketch framework.

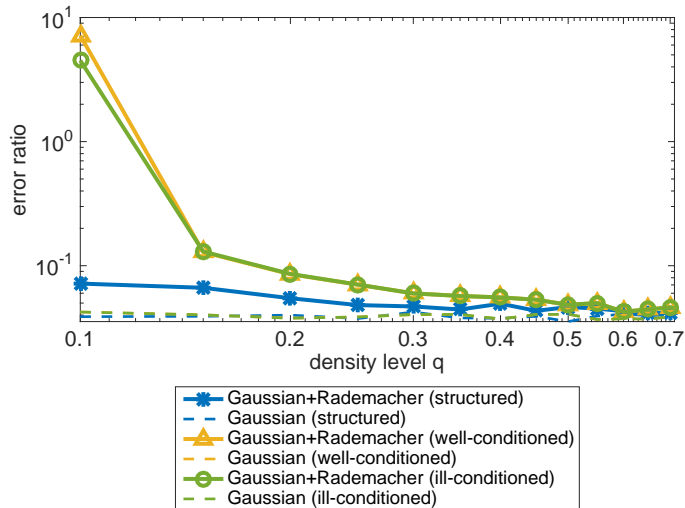


Figure 3: We compare the performance of the G+R sketching strategy with varying density level q and the fixed sketching dimension $m = 400$ on three different regression problems. The size of the regressions is set as $n_1 n_2 = 64^2$ by $p = 15$. We add the standard dense Gaussian matrices on the same regression problems for reference.

In Figure 4, for the well-conditioned linear regression only, we test three sketching strategies: G+R, G+G and R+R. All three curves seem to be parallel to that of the standard Gaussian and Rademacher sketching matrices. We can clearly see the impact of the constant factor $(\mathcal{M}^2 + 1)$ in these three curves: the R+R curve has smaller error ratios because it has bounded magnitude in the tensor factors of the sketching matrix. We thus conclude that the magnitude in the tensor-structured sketch does affect the sketching quality and the bounded assumption in the theory statement is necessary.

6 Conclusions and future work

In this paper, motivated by structured least squares in practical applications, we presented a row-wise tensor-structured sketching design to accelerate the solving procedure. We have demonstrated a state-of-the-art estimate for the sketching dimension of the proposed sketch in terms of the Gaussian width. The result directly applies to common types of optimizations in different geometry landscapes. In light of the theoretical support to the main result, we developed the analysis for the maximum embedding error of the proposed sketching matrix over a fixed set, with the help of the generic chaining technique. We ran numerical simulations and showed that the empirical results are consistent with the theory.

Future work remains, first, extending the current result in the order-2 case to higher order tensor structure. Secondly, the sketching model in this work considers only the sub-Gaussian random variables, an interesting open problem would be analyzing the sketching property for the randomized FFT-related construction with tensor structure, as such class of sketch enables fast matrix-vector multiplications. The last open problem is inspired by the numerical observations shown in figures 1 to 3, that the proposed sketching design works better on the tensor-structured programs than unstructured programs. This may suggest that a tighter sketching size estimate

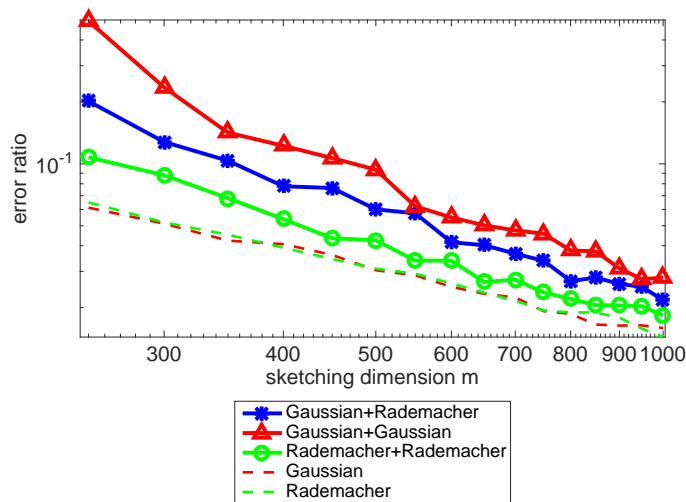


Figure 4: We compare the sketching performances of the G+R, G+G and R+R sketchings with varying sketching size m on a well-conditioned linear regression problem of size $n_1 n_2 = 64^2$ by $p = 15$. All three types of random sketches are constructed with density level $q = 0.2$. In addition, we implement the standard Gaussian and Rademacher matrices on the same program for reference.

could be derived for tensor-structured programs.

Acknowledgements

The authors would like to thank Rachel Ward for her insights and helpful discussions. Chen is supported by the Office of Naval Research (award N00014-18-1-2354) and by the National Science Foundation (awards 1952735 and 1620472).

References

- [1] Nir Ailon and Bernard Chazelle. Approximate nearest neighbors and the fast Johnson-Lindenstrauss transform. In *STOC'06: Proceedings of the 38th Annual ACM Symposium on Theory of Computing*, pages 557–563. ACM, New York, 2006.
- [2] Animashree Anandkumar, Rong Ge, Daniel Hsu, Sham M. Kakade, and Matus Telgarsky. Tensor decompositions for learning latent variable models. *Journal of Machine Learning Research*, 15:2773–2832, 2014.
- [3] Haim Avron, Huy Nguyen, and David Woodruff. Subspace embeddings for the polynomial kernel. In *Advances in Neural Information Processing Systems 27*, pages 2258–2266. Curran Associates, Inc., 2014.
- [4] Mohammad Taha Bahadori, Qi (Rose) Yu, and Yan Liu. Fast multivariate spatio-temporal analysis via low rank tensor learning. In *Advances in Neural Information Processing Systems 27*, pages 3491–3499. Curran Associates, Inc., 2014.

- [5] Peter L Bartlett, Olivier Bousquet, and Shahar Mendelson. Local rademacher complexities. *The Annals of Statistics*, 33(4):1497–1537, 2005.
- [6] Casey Battaglino, Grey Ballard, and Tamara G. Kolda. A practical randomized CP tensor decomposition. *SIAM J. Matrix Anal. Appl.*, 39(2):876–901, 2018.
- [7] Léon Bottou, Frank E. Curtis, and Jorge Nocedal. Optimization methods for large-scale machine learning. *SIAM Review*, 60(2):223–311, 2018.
- [8] Sébastien Bubeck. Convex optimization: Algorithms and complexity. *Foundations and Trends in Machine Learning*, 8(3-4):231–357, 2015.
- [9] Moses Charikar, Kevin C. Chen, and Martin Farach-Colton. Finding frequent items in data streams. *Theor. Comput. Sci.*, 312(1):3–15, 2004.
- [10] Ke Chen, Qin Li, Kit Newton, and Steve Wright. Structured random sketching for PDE inverse problems. *arXiv e-prints*, September 2019.
- [11] Dehua Cheng, Richard Peng, Yan Liu, and Ioakeim Perros. SPALS: fast alternating least squares via implicit leverage scores sampling. In *Advances in Neural Information Processing Systems 29: Annual Conference on Neural Information Processing Systems 2016, December 5-10, 2016, Barcelona, Spain*, pages 721–729, 2016.
- [12] Kenneth L. Clarkson and David P. Woodruff. Low rank approximation and regression in input sparsity time. In *Proceedings of the Forty-fifth Annual ACM Symposium on Theory of Computing*, STOC '13, pages 81–90, New York, NY, USA, 2013. ACM.
- [13] Nadav Cohen, Or Sharir, and Amnon Shashua. On the expressive power of deep learning: A tensor analysis. volume 49 of *Proceedings of Machine Learning Research*, pages 698–728, Columbia University, New York, New York, USA, 23–26 Jun 2016. PMLR.
- [14] Anirban Dasgupta, Ravi Kumar, and Tamás Sarlós. A sparse Johnson-Lindenstrauss transform. In *STOC'10—Proceedings of the 2010 ACM International Symposium on Theory of Computing*, pages 341–350. ACM, New York, 2010.
- [15] Lieven De Lathauwer, Bart De Moor, and Joos Vandewalle. A multilinear singular value decomposition. *SIAM Journal on Matrix Analysis and Applications*, 21(4):1253–1278, 2000.
- [16] Huaian Diao, Zhao Song, Wen Sun, and David P. Woodruff. Sketching for Kronecker Product Regression and P-splines. In *International Conference on Artificial Intelligence and Statistics, AISTATS*, pages 1299–1308, 2018.
- [17] Petros Drineas, Michael W. Mahoney, and S. Muthukrishnan. Sampling algorithms for l2 regression and applications, 2006.
- [18] M. A. T. Figueiredo, R. D. Nowak, and S. J. Wright. Gradient projection for sparse reconstruction: Application to compressed sensing and other inverse problems. *IEEE Journal of Selected Topics in Signal Processing*, 1(4):586–597, 2007.
- [19] Peter D. Hoff. Multilinear tensor regression for longitudinal relational data. *Ann. Appl. Stat.*, 9(3):1169–1193, 09 2015.

- [20] Ruhui Jin, Tamara G. Kolda, and Rachel Ward. Fast Johnson-Lindenstrauss transforms via Kronecker products. *arXiv e-prints*, September 2019.
- [21] William B. Johnson and Joram Lindenstrauss. Extensions of Lipschitz mappings into a Hilbert space. volume 26 of *Contemp. Math.*, pages 189–206. Amer. Math. Soc., Providence, RI, 1984.
- [22] Purushottam Kar and Harish Karnick. Random feature maps for dot product kernels. volume 22 of *Proceedings of Machine Learning Research*, pages 583–591, La Palma, Canary Islands, 21–23 Apr 2012. PMLR.
- [23] B. Klartag and S. Mendelson. Empirical processes and random projections. *Journal of Functional Analysis*, 225(1):229 – 245, 2005.
- [24] T. Kolda and B. Bader. Tensor decompositions and applications. *SIAM Review*, 51(3):455–500, 2009.
- [25] Xingguo Li, Jarvis Haupt, and David Woodruff. Near optimal sketching of low-rank tensor regression. In *Advances in Neural Information Processing Systems 30*, pages 3466–3476. Curran Associates, Inc., 2017.
- [26] Osman A. Malik and Stephen Becker. Guarantees for the kronecker fast johnson-lindenstrauss transform using a coherence and sampling argument. *Linear Algebra and its Applications*, 602:120–137, October 2020.
- [27] Michela Meister, Tamas Sarlos, and David Woodruff. Tight dimensionality reduction for sketching low degree polynomial kernels. In H. Wallach, H. Larochelle, A. Beygelzimer, F. dAlché Buc, E. Fox, and R. Garnett, editors, *Advances in Neural Information Processing Systems 32*, pages 9475–9486. Curran Associates, Inc., 2019.
- [28] Shahar Mendelson, Alain Pajor, and Nicole Tomczak-Jaegermann. Reconstruction and subgaussian operators in asymptotic geometric analysis. *Geometric and Functional Analysis*, 17:1248–1282, 11 2007.
- [29] Xiangrui Meng and Michael W. Mahoney. Low-distortion subspace embeddings in input-sparsity time and applications to robust linear regression. In *Proceedings of the 45th Annual ACM Symposium on Theory of Computing*, pages 91–100. ACM, 2013.
- [30] J. Nelson. Chaining introduction with some computer science applications. *Bull. EATCS*, 120, 2016.
- [31] Jorge Nocedal and Stephen J. Wright. *Numerical optimization*. Springer series in operations research and financial engineering. Springer, New York, NY, 2. ed. edition, 2006.
- [32] G. Ortiz-Jimenez, M. Coutino, S. P. Chepuri, and G. Leus. Sparse sampling for inverse problems with tensors. *IEEE Transactions on Signal Processing*, 67(12):3272–3286, 2019.
- [33] Rasmus Pagh. Compressed matrix multiplication. *ACM Transactions on Computation Theory*, 5, 08 2011.

- [34] Ninh Pham and Rasmus Pagh. Fast and scalable polynomial kernels via explicit feature maps. In *Proceedings of the 19th ACM SIGKDD International Conference on Knowledge Discovery and Data Mining*, KDD '13, pages 239–247, New York, NY, USA, 2013. ACM.
- [35] M. Pilanci and M. J. Wainwright. Randomized sketches of convex programs with sharp guarantees. *IEEE Transactions on Information Theory*, 61(9):5096–5115, 2015.
- [36] Mert Pilanci and Martin J. Wainwright. Iterative hessian sketch: Fast and accurate solution approximation for constrained least-squares. *Journal of Machine Learning Research*, 17(53):1–38, 2016.
- [37] Beheshteh T. Rakhshan and Guillaume Rabusseau. Tensorized Random Projections. *arXiv e-prints*, page arXiv:2003.05101, March 2020.
- [38] Vladimir Rokhlin and Mark Tygert. A fast randomized algorithm for overdetermined linear least-squares regression. *Proceedings of the National Academy of Sciences*, 105(36):13212–13217, 2008.
- [39] Mark Rudelson and Roman Vershynin. On sparse reconstruction from Fourier and Gaussian measurements. *Comm. Pure Appl. Math.*, 61(8):1025–1045, 2008.
- [40] Yiming Sun, Yang Guo, Joel A Tropp, and Madeleine Udell. Tensor random projection for low memory dimension reduction. In *NeurIPS Workshop on Relational Representation Learning*, 2018.
- [41] M. Talagrand. *The Generic Chaining: Upper and Lower Bounds of Stochastic Processes*. Springer Monographs in Mathematics. Springer Berlin Heidelberg, 2005.
- [42] Michel Talagrand. Majorizing measures: the generic chaining. *Ann. Probab.*, 24(3):1049–1103, 07 1996.
- [43] Robert Tibshirani. Regression shrinkage and selection via the lasso. *Journal of the Royal Statistical Society. Series B (Methodological)*, 58(1):267–288.
- [44] Joel A. Tropp. Improved analysis of the subsampled randomized hadamard transform. *Adv. Data Sci. Adapt. Anal.*, 3(1-2):115–126, 2011.
- [45] Roman Vershynin. Estimation in high dimensions: A geometric perspective. *Applied and Numerical Harmonic Analysis*, 05 2014.
- [46] Roman Vershynin. *High-Dimensional Probability: An Introduction with Applications in Data Science*. 09 2018.
- [47] Shuheng Zhou. Sparse hanson-wright inequalities for subgaussian quadratic forms. *Bernoulli*, 25(3):1603–1639, 08 2019.

A Proof of Lemma 3.3

1. *Estimation of D_1 .* By letting $\mathcal{Y} = \mathbf{AK}$, since $m \geq \frac{C_2 \mathbb{W}(\overline{\mathbf{AK}})^2}{q^2}$, Theorem 3.1 implies that with probability at least $1 - 4 \exp(-cm \frac{\omega^2 q}{2})$,

$$1 - \inf_{\mathbf{y} \in \overline{\mathbf{AK}}} \|\mathbf{S}\mathbf{y}\|_2^2 \leq \sup_{\mathbf{y} \in \overline{\mathbf{AK}}} \left| \|\mathbf{S}\mathbf{y}\|_2^2 - 1 \right| \leq \theta \left(\frac{C_1 \mathbb{W}(\overline{\mathcal{Y}})}{\sqrt{m}q} + \omega \right).$$

We complete the proof for D_1 by adjusting the above inequality to (25). \square

2. *Estimation of D_2 .* The proof follows the same logic as Lemma 3 in [35]. Here we provide the essential part of the proof and omit repetitive details from [35].

We use short-hand notations: $\mathbf{M} = \mathbf{S}^\top \mathbf{S} - \mathbf{I}_{n_1 n_2} \in \mathbb{R}^{n_1 n_2 \times n_1 n_2}$, $\mathbf{z} = \frac{\mathbf{Ax}^* - \mathbf{b}}{\|\mathbf{Ax}^* - \mathbf{b}\|_2} \in \mathcal{S}^{n_1 n_2 - 1}$, and $\tilde{\mathbf{y}} = \frac{\mathbf{y}}{\|\mathbf{y}\|_2} \in \overline{\mathbf{AK}}$. Consider two subsets of $\mathbf{AK} \subset \mathbb{R}^{n_1 n_2}$:

$$\mathbf{AK}_+ = \{\mathbf{y} \in \mathbf{AK} \mid \langle \mathbf{z}, \mathbf{y} \rangle \geq 0\}, \quad \mathbf{AK}_- = \{\mathbf{y} \in \mathbf{AK} \mid \langle \mathbf{z}, \mathbf{y} \rangle < 0\}.$$

Then

$$D_2 = \sup_{\mathbf{y} \in \mathbf{AK}} |\tilde{\mathbf{y}}^\top \mathbf{M}\mathbf{z}| = \max \left(\sup_{\mathbf{y} \in \mathbf{AK}_+} |\tilde{\mathbf{y}}^\top \mathbf{M}\mathbf{z}|, \sup_{\mathbf{y} \in \mathbf{AK}_-} |\tilde{\mathbf{y}}^\top \mathbf{M}\mathbf{z}| \right). \quad (50)$$

In the case of $\sup_{\mathbf{y} \in \mathbf{AK}_+} |\tilde{\mathbf{y}}^\top \mathbf{M}\mathbf{z}|$, we show its partition

$$\sup_{\mathbf{y} \in \mathbf{AK}_+} |\tilde{\mathbf{y}}^\top \mathbf{M}\mathbf{z}| \leq \frac{1}{2} \left(\sup_{\mathbf{y} \in \mathbf{AK}_+} |(\tilde{\mathbf{y}} + \mathbf{z})^\top \mathbf{M}(\tilde{\mathbf{y}} + \mathbf{z})| + \sup_{\mathbf{y} \in \mathbf{AK}_+} |\tilde{\mathbf{y}}^\top \mathbf{M}\tilde{\mathbf{y}}| + \sup_{\mathbf{y} \in \mathbf{AK}_+} |\mathbf{z}^\top \mathbf{M}\mathbf{z}| \right). \quad (51)$$

We apply Theorem 3.1 three times to respectively bound each term on the right-hand side of (51). From Lemma 3's proof result equation (55) in [35], we can establish

$$\sup_{\mathbf{y} \in \mathbf{AK}_+} |\tilde{\mathbf{y}}^\top \mathbf{M}\mathbf{z}| \leq \theta \left(5 \frac{C_1 \mathbb{W}(\overline{\mathbf{AK}})}{\sqrt{m}q} + 3\omega \right), \quad (52)$$

with failure probability less than three times of the failure probability in Theorem 3.1, that is $12 \exp(-cm \frac{\omega^2 q}{2})$.

We can obtain the same bound for $\sup_{\mathbf{y} \in \mathbf{AK}_-} |\tilde{\mathbf{y}}^\top \mathbf{M}\mathbf{z}|$ following a similar argument for $\sup_{\mathbf{y} \in \mathbf{AK}_+} |\tilde{\mathbf{y}}^\top \mathbf{M}\mathbf{z}|$. Taking a union of the failure of each term in (50) being well controlled, we can conclude the proof by

$$D_2 = \sup_{\mathbf{y} \in \mathbf{AK}} |\tilde{\mathbf{y}}^\top \mathbf{M}\mathbf{z}| \leq \theta \left(5 \frac{C_1 \mathbb{W}(\overline{\mathbf{AK}})}{\sqrt{m}q} + 3\omega \right), \quad (53)$$

achieves with probability exceeding $1 - 24 \exp(-cm \frac{\omega^2 q}{2})$. \square

B Proof of Proposition 4.1

Proof. The core of Proposition 4.1 is deriving the moment generating function for one quadratic form by each process \mathbf{s}_k . In particular, there exist two constants $c_1, c_2 > 0$, for each $k \in [m]$, if $|\lambda| \leq \frac{c_1}{\beta^2 \|\mathbf{A}_k\|_2}$, then

$$\begin{aligned} \mathbb{E} \exp(\lambda (\mathbf{s}_k^\top \mathbf{A}_k \mathbf{s}_k - \mathbb{E} \mathbf{s}_k^\top \mathbf{A}_k \mathbf{s}_k)) &\leq \exp(c_2 \lambda^2 \beta^4 (q \|\text{diag}(\mathbf{A}_k)\|_F^2 + q^2 \|\text{off}(\mathbf{A}_k)\|_F^2)) \\ &\leq \exp(c_2 \lambda^2 \beta^4 q \|\mathbf{A}_k\|_F^2). \end{aligned} \quad (54)$$

We refer the readers to the proof of Lemma 3.1 and equation (9) in [47] specifically for the diagonal and off-diagonal parts of the MGF. We add the two parts along with the condition on $|\lambda| \leq \frac{c_1}{\beta^2 \|\mathbf{A}_k\|_2}$ and yield (54). Note to simplify the MGF bound, we combine the diagonal and off-diagonal Frobenius norms and obtain an upper bound depending on the overall Frobenius norm.

We proceed to consider the performance of the averaged chaos from independent processes. Denote

$$W = \sum_{k=1}^m \frac{1}{m} (\mathbf{s}_k^\top \mathbf{A}_k \mathbf{s}_k - \mathbb{E} \mathbf{s}_k^\top \mathbf{A}_k \mathbf{s}_k),$$

and $K_1 = \max_{k \in [m]} \|\mathbf{A}_k\|_2, K_2 = \max_{k \in [m]} \|\mathbf{A}_k\|_F$. Since each process \mathbf{s}_k is independent, we apply the MGF bound (54), if $\frac{|\lambda|}{m} \leq \frac{c_1}{\beta^2 K_1}$,

$$\begin{aligned} \mathbb{E} \exp(\lambda W) &= \prod_{k=1}^m \mathbb{E} \exp\left(\lambda \frac{1}{m} (\mathbf{s}_k^\top \mathbf{A}_k \mathbf{s}_k - \mathbb{E} \mathbf{s}_k^\top \mathbf{A}_k \mathbf{s}_k)\right) \\ &\leq \prod_{k=1}^m \exp\left(c_2 \lambda^2 \frac{1}{m^2} \beta^4 q \|\mathbf{A}_k\|_F^2\right) = \exp\left(c_2 \lambda^2 \frac{1}{m^2} \beta^4 q \sum_{k=1}^m \|\mathbf{A}_k\|_F^2\right) \\ &\leq \exp\left(c_2 \lambda^2 \beta^4 \frac{1}{m} K_2^2 q\right). \end{aligned}$$

For $t > 0$, by Markov's inequality,

$$\begin{aligned} \Pr(W > t) &= \Pr(\exp(\lambda W) > \exp(\lambda t)) \\ &\leq \frac{\mathbb{E} \exp(\lambda W)}{\exp(\lambda t)} \leq \exp\left(-\lambda t + c_2 \lambda^2 \beta^4 \frac{1}{m} K_2^2 q\right). \end{aligned} \quad (55)$$

We choose the value of λ :

$$\lambda = \min\left(\frac{c_1 m}{\beta^2 K_1}, \frac{m t}{2 c_2 \beta^4 K_2^2 q}\right), \quad (56)$$

to further optimize (55), then

$$\Pr(W > t) \leq \exp\left(-\min\left(\frac{c_1 m t}{2 \beta^2 K_1}, \frac{m t^2}{4 c_2 \beta^4 K_2^2 q}\right)\right).$$

Since $\Pr(|W| > t) = \Pr(W > t) + \Pr(W < -t)$ and the MGF bound is symmetric regarding to λ , we can derive the same bound for $\Pr(W < -t)$.

By setting $c = \min\left(\frac{c_1}{2}, \frac{1}{4c_2}\right)$, we can finalize the result

$$\Pr\left(\left|\frac{1}{m} \sum_{k=1}^m \mathbf{s}_k^\top \mathbf{A}_k \mathbf{s}_k - \mathbb{E} \mathbf{s}_k^\top \mathbf{A}_k \mathbf{s}_k\right| > t\right) = \Pr(|W| > t) \leq 2 \exp\left(-c m \min\left(\frac{t}{K_1 \beta^2}, \frac{t^2}{K_2^2 \beta^4 q}\right)\right).$$

□

C Proof of Lemma 4.2

Proof. Before we dig into the proof for each case, we introduce the general structure that is used for all three cases. The idea is to analyze the randomness of $\boldsymbol{\eta} \in \mathbb{R}^{n_1}$ and $\boldsymbol{\xi} \in \mathbb{R}^{n_2}$ separately. The detailed methods are as follows.

First, we consider as $\boldsymbol{\eta}$ random but $\boldsymbol{\xi}$ as deterministic. We define a linear map for every $k \in [m]$, $\mathbf{Z}_k = \mathbf{I}_{n_1} \otimes \boldsymbol{\xi}_k^\top = \text{diag}(\boldsymbol{\xi}_k^\top) \in \mathbb{R}^{n_1 \times n_1 n_2}$. Note that for a fixed $\mathbf{y} \in \mathcal{Y} \subset \mathcal{S}^{n_1 n_2 - 1}$, $\langle \boldsymbol{\eta}_k \otimes \boldsymbol{\xi}_k, \mathbf{y} \rangle = \langle \boldsymbol{\eta}_k, \mathbf{Z}_k \mathbf{y} \rangle$. Because $\boldsymbol{\eta}_k$ is isotropic, we have $\mathbb{E}_{\boldsymbol{\eta}} \langle \boldsymbol{\eta}_k, \mathbf{Z}_k \mathbf{y} \rangle^2 = \|\mathbf{Z}_k \mathbf{y}\|_2^2$, and

$$\frac{1}{m} \sum_{k=1}^m \langle \boldsymbol{\eta}_k, \mathbf{Z}_k \mathbf{y} \rangle^2 - \|\mathbf{Z}_k \mathbf{y}\|_2^2 \quad (57)$$

is a zero-mean random variable with randomness coming from $\boldsymbol{\eta}$, if we treat \mathbf{Z}_k as deterministic construction.

We now take the randomness from $\boldsymbol{\xi}$ into account. We denote the block partition of \mathbf{y} with each block vector \mathbf{y}_i of length n_2 : $\mathbf{y} = [\mathbf{y}_1^\top, \mathbf{y}_2^\top, \dots, \mathbf{y}_{n_1}^\top]^\top \in \mathbb{R}^{n_1 n_2}$. Since $\boldsymbol{\xi}_k$ is isotropic, for $k \in [m]$, $\mathbb{E} \sum_{i=1}^{n_1} \langle \boldsymbol{\xi}_k, \mathbf{y}_i \rangle^2 = \sum_{i=1}^{n_1} \|\mathbf{y}_i\|_2^2 = \|\mathbf{y}\|_2^2$, thus

$$\left(\frac{1}{m} \sum_{k=1}^m \sum_{i=1}^{n_1} \langle \boldsymbol{\xi}_k, \mathbf{y}_i \rangle^2\right) - \|\mathbf{y}\|_2^2 \quad (58)$$

is also a zero-mean random variable. Additionally, we notice that

$$\|\mathbf{Z}_k \mathbf{y}\|_2^2 = \sum_{i=1}^{n_1} \langle \boldsymbol{\xi}_k, \mathbf{y}_i \rangle^2. \quad (59)$$

Therefore we can divide the distortion as follows:

$$\left(\frac{1}{m} \sum_{k=1}^m \langle \boldsymbol{\eta}_k \otimes \boldsymbol{\xi}_k, \mathbf{y} \rangle^2\right) - \|\mathbf{y}\|_2^2 = \underbrace{\left(\frac{1}{m} \sum_{k=1}^m \langle \boldsymbol{\eta}_k, \mathbf{Z}_k \mathbf{y} \rangle^2 - \|\mathbf{Z}_k \mathbf{y}\|_2^2\right)}_{(57)} + \underbrace{\left(\left(\frac{1}{m} \sum_{k=1}^m \sum_{i=1}^{n_1} \langle \boldsymbol{\xi}_k, \mathbf{y}_i \rangle^2\right) - \|\mathbf{y}\|_2^2\right)}_{(58)}. \quad (60)$$

We proceed to the detailed proofs for case 1, 2 and 3.

1. Let $\mathbf{B}_k = \mathbf{Z}_k \mathbf{y} \mathbf{y}^\top \mathbf{Z}_k^\top \in \mathbb{R}^{n_1 \times n_1}$, then

$$\frac{1}{m} \sum_{k=1}^m \langle \boldsymbol{\eta}_k, \mathbf{Z}_k \mathbf{y} \rangle^2 - \|\mathbf{Z}_k \mathbf{y}\|_2^2 = \frac{1}{m} \sum_{k=1}^m \boldsymbol{\eta}_k^\top \mathbf{B}_k \boldsymbol{\eta}_k - \mathbb{E} \boldsymbol{\eta}_k^\top \mathbf{B}_k \boldsymbol{\eta}_k.$$

As $\|\mathbf{Z}_k\|_2 = \sqrt{\lambda_{\max}(\mathbf{Z}_k^\top \mathbf{Z}_k)} = \|\boldsymbol{\xi}_k\|_\infty \leq \mathcal{M}$, and \mathbf{B}_k is a rank-1 matrix, we have

$$\|\mathbf{B}_k\|_2 = \|\mathbf{B}_k\|_F \leq \|\mathbf{Z}_k \mathbf{y}\|_2^2 \leq \|\mathbf{Z}_k\|_2^2 \|\mathbf{y}\|_2^2 \leq \mathcal{M}^2.$$

Each element's ψ_2 norm in $\boldsymbol{\eta}$ is bounded by α/\sqrt{q} , we apply Proposition 4.1 by setting

$$\beta = \frac{\alpha}{\sqrt{q}}, \quad t = u \alpha^2 \mathcal{M}^2, \quad \mathbf{A}_k = \mathbf{B}_k.$$

As the spectral bounds as $K_1 = K_2 \leq \mathcal{M}^2$, for every $u > 0$,

$$\begin{aligned} \Pr \left(\left| \frac{1}{m} \sum_{k=1}^m \langle \boldsymbol{\eta}_k, \mathbf{Z}_k \mathbf{y} \rangle^2 - \|\mathbf{Z}_k \mathbf{y}\|_2^2 \right| \geq u \alpha^2 \mathcal{M}^2 \right) &= \Pr \left(\left| \frac{1}{m} \sum_{k=1}^m \boldsymbol{\eta}_k^\top \mathbf{B}_k \boldsymbol{\eta}_k - \mathbb{E} \boldsymbol{\eta}_k^\top \mathbf{B}_k \boldsymbol{\eta}_k \right| \geq u \alpha^2 \mathcal{M}^2 \right) \\ &\leq 2 \exp \left(-cm \min \left(\frac{u \alpha^2 \mathcal{M}^2}{\frac{\alpha^2}{q} \mathcal{M}^2}, \frac{(u \alpha^2 \mathcal{M}^2)^2}{q \frac{\alpha^4}{q^2} \mathcal{M}^4} \right) \right) = 2 \exp \left(-cm \min (u q, u^2 q) \right). \end{aligned} \quad (61)$$

This provides a tail bound for the first term (57) in the right-hand side of (60), to deal with the second term (58), let $\mathbf{B} = \sum_{i=1}^{n_1} \mathbf{y}_i \mathbf{y}_i^\top \in \mathbb{R}^{n_2 \times n_2}$, (58) can be written as

$$\frac{1}{m} \sum_{k=1}^m \sum_{i=1}^{n_1} \langle \boldsymbol{\xi}_k, \mathbf{y}_i \rangle^2 - \|\mathbf{y}\|_2^2 = \frac{1}{m} \sum_{k=1}^m \boldsymbol{\xi}_k^\top \mathbf{B} \boldsymbol{\xi}_k - \mathbb{E} \boldsymbol{\xi}_k^\top \mathbf{B} \boldsymbol{\xi}_k.$$

Since \mathbf{B} is a sum of rank-1 matrices $\mathbf{y}_i \mathbf{y}_i^\top$,

$$\|\mathbf{B}\|_2 \leq \|\mathbf{B}\|_F \leq \sum_{i=1}^{n_1} \|\mathbf{y}_i \mathbf{y}_i^\top\|_2 = \sum_{i=1}^{n_1} \|\mathbf{y}_i\|_2^2 = \|\mathbf{y}\|_2^2 = 1.$$

Each element's ψ_2 norm in $\boldsymbol{\xi}$ is bounded by α/\sqrt{q} , we can again apply Proposition 4.1,

$$\begin{aligned} \Pr \left(\left| \frac{1}{m} \sum_{k=1}^m \sum_{i=1}^{n_1} \langle \boldsymbol{\xi}_k, \mathbf{y}_i \rangle^2 - \|\mathbf{y}\|_2^2 \right| \geq u \alpha^2 \right) &= \Pr \left(\left| \frac{1}{m} \sum_{k=1}^m \boldsymbol{\xi}_k^\top \mathbf{B} \boldsymbol{\xi}_k - \mathbb{E} \boldsymbol{\xi}_k^\top \mathbf{B} \boldsymbol{\xi}_k \right| \geq u \alpha^2 \right) \\ &\leq 2 \exp \left(-cm \min \left(\frac{u \alpha^2}{\frac{\alpha^2}{q}}, \frac{(u \alpha^2)^2}{\frac{\alpha^4}{q}} \right) \right) = 2 \exp \left(-cm \min (u q, u^2 q) \right). \end{aligned} \quad (62)$$

As the probability for $Q(\mathbf{y})$ can be bounded by two partitions given in (60),

$$\begin{aligned} \Pr(|Q(\mathbf{y})| \geq u\alpha^2(\mathcal{M}^2 + 1)) &\leq \Pr\left(\left|\frac{1}{m}\sum_{k=1}^m \langle \boldsymbol{\eta}_k, \mathbf{Z}_{2,k} \mathbf{y} \rangle^2 - \|\mathbf{Z}_{2,k} \mathbf{y}\|_2^2\right| \geq u\alpha^2 \mathcal{M}^2\right) \\ &\quad + \Pr\left(\left|\frac{1}{m}\sum_{k=1}^m \sum_{i=1}^{n_1} \langle \boldsymbol{\xi}_k, \mathbf{y}_i \rangle^2 - \|\mathbf{y}\|_2^2\right| \geq u\alpha^2\right), \end{aligned}$$

we use the results from (61) and (62), and continue from the above inequality,

$$\Pr(|Q(\mathbf{y})| \geq u\alpha^2(\mathcal{M}^2 + 1)) \leq 4 \exp(-cm \min(uq, u^2q)).$$

2. To prove case 2, we imitate the procedures in proving case 1, while the major difference is deriving the spectral results of the centered matrices of the quadratic forms.

First, recalling (60), we can divide the target term $Q(\mathbf{y}) - Q(\mathbf{y}')$ into two parts,

$$\begin{aligned} Q(\mathbf{y}) - Q(\mathbf{y}') &= \left(\frac{1}{m}\sum_{k=1}^m \langle \boldsymbol{\eta}_k, \mathbf{Z}_k \mathbf{y} \rangle^2 - \langle \boldsymbol{\eta}_k, \mathbf{Z}_k \mathbf{y}' \rangle^2\right) - \left(\frac{1}{m}\sum_{k=1}^m \|\mathbf{Z}_k \mathbf{y}\|_2^2 - \|\mathbf{Z}_k \mathbf{y}'\|_2^2\right) \\ &\quad + \left(\frac{1}{m}\sum_{k=1}^m \sum_{i=1}^{n_1} \langle \boldsymbol{\xi}_k, \mathbf{y}_i \rangle^2 - \frac{1}{m}\sum_{k=1}^m \sum_{i=1}^{n_1} \langle \boldsymbol{\xi}_k, \mathbf{y}'_i \rangle^2\right) - (\|\mathbf{y}\|_2^2 - \|\mathbf{y}'\|_2^2). \end{aligned} \tag{63}$$

If we define

$$\mathbf{C}_k = \mathbf{Z}_k (\mathbf{y} \mathbf{y}^\top - \mathbf{y}' \mathbf{y}'^\top) \mathbf{Z}_k^\top \in \mathbb{R}^{n_1 \times n_1}, \quad \mathbf{C} = \sum_{i=1}^{n_1} \mathbf{y}_i \mathbf{y}_i^\top - \mathbf{y}'_i \mathbf{y}'_i^\top \in \mathbb{R}^{n_2 \times n_2},$$

(63) can then be written in a compact form,

$$Q(\mathbf{y}) - Q(\mathbf{y}') = \left(\frac{1}{m}\sum_{k=1}^m \boldsymbol{\eta}_k^\top \mathbf{C}_k \boldsymbol{\eta}_k - \mathbb{E} \boldsymbol{\eta}_k^\top \mathbf{C}_k \boldsymbol{\eta}_k\right) + \left(\frac{1}{m}\sum_{k=1}^m \boldsymbol{\xi}_k^\top \mathbf{C} \boldsymbol{\xi}_k - \mathbb{E} \boldsymbol{\xi}_k^\top \mathbf{C} \boldsymbol{\xi}_k\right). \tag{64}$$

Next, we derive the spectral results for the centered matrices \mathbf{C}_k, \mathbf{C} . As

$$\mathbf{C}_k = \mathbf{Z}_k (\mathbf{y} \mathbf{y}^\top - \mathbf{y}' \mathbf{y}'^\top) \mathbf{Z}_k^\top = \frac{1}{2} \mathbf{Z}_k [(\mathbf{y} - \mathbf{y}')(\mathbf{y} + \mathbf{y}')^\top + (\mathbf{y} + \mathbf{y}')(\mathbf{y} - \mathbf{y}')^\top] \mathbf{Z}_k^\top,$$

the spectral results yield

$$\begin{aligned} \|\mathbf{C}_k\|_2 \leq \|\mathbf{C}_k\|_F &\leq \frac{1}{2} \|\mathbf{Z}_k (\mathbf{y} - \mathbf{y}')(\mathbf{y} + \mathbf{y}')^\top \mathbf{Z}_k^\top\|_2 + \frac{1}{2} \|\mathbf{Z}_k (\mathbf{y} + \mathbf{y}')(\mathbf{y} - \mathbf{y}')^\top \mathbf{Z}_k^\top\|_2 \\ &\leq \|\mathbf{Z}_k\|_2^2 \|\mathbf{y} + \mathbf{y}'\|_2 \|\mathbf{y} - \mathbf{y}'\|_2 \leq \mathcal{M}^2 \sqrt{2} \|\mathbf{y} - \mathbf{y}'\|_2. \end{aligned}$$

The last step is because $\|\mathbf{Z}_k\|_2 \leq \mathcal{M}$ and \mathbf{y}, \mathbf{y}' are on the unit sphere, $\|\mathbf{y} + \mathbf{y}'\|_2 \leq \sqrt{2}$.

Similarly, for $\mathbf{C} \in \mathbb{R}^{n_2 \times n_2}$, since

$$\mathbf{C} = \sum_{i=1}^{n_1} \mathbf{y}_i \mathbf{y}_i^\top - \mathbf{y}'_i \mathbf{y}'_i{}^\top = \frac{1}{2} \sum_{i=1}^{n_1} (\mathbf{y}_i - \mathbf{y}'_i) (\mathbf{y}_i + \mathbf{y}'_i)^\top + (\mathbf{y}_i + \mathbf{y}'_i) (\mathbf{y}_i - \mathbf{y}'_i)^\top,$$

then

$$\begin{aligned} \|\mathbf{C}\|_2 \leq \|\mathbf{C}\|_F &= \sum_{i=1}^{n_1} \|\mathbf{y}_i - \mathbf{y}'_i\|_2 \|\mathbf{y}_i + \mathbf{y}'_i\|_2 \leq \sqrt{\sum_{i=1}^{n_1} \|\mathbf{y}_i - \mathbf{y}'_i\|_2^2} \sqrt{\sum_{i=1}^{n_1} \|\mathbf{y}_i + \mathbf{y}'_i\|_2^2} \\ &= \|\mathbf{y} - \mathbf{y}'\|_2 \|\mathbf{y} + \mathbf{y}'\|_2 \leq \sqrt{2} \|\mathbf{y} - \mathbf{y}'\|_2, \end{aligned}$$

we have that $\|\mathbf{C}\|_2 \leq \|\mathbf{C}\|_F \leq \sqrt{2} \|\mathbf{y} - \mathbf{y}'\|_2$.

Then, for $\mathbf{y}, \mathbf{y}' \in \mathcal{S}^{n_1 n_2 - 1}$, we again apply Proposition 4.1, by setting

$$\beta = \frac{\alpha}{\sqrt{q}}, \quad t = u \alpha^2 (\mathcal{M}^2 + 1) \|\mathbf{y} - \mathbf{y}'\|_2, \quad \mathbf{A}_k = \mathbf{C}_k, \quad \mathbf{C}.$$

Then we can take a union bound by (64),

$$\begin{aligned} &\Pr(|Q(\mathbf{y}) - Q(\mathbf{y}')| \geq u \alpha^2 (\mathcal{M}^2 + 1) \|\mathbf{y} - \mathbf{y}'\|_2) \\ &\leq \Pr\left(\left|\frac{1}{m} \sum_{k=1}^m \boldsymbol{\eta}_k^\top \mathbf{C}_k \boldsymbol{\eta}_k - \mathbb{E} \boldsymbol{\eta}_k^\top \mathbf{C}_k \boldsymbol{\eta}_k\right| \geq u \alpha^2 \mathcal{M}^2 \|\mathbf{y} - \mathbf{y}'\|_2\right) \\ &+ \Pr\left(\left|\frac{1}{m} \sum_{k=1}^m \boldsymbol{\xi}_k^\top \mathbf{C} \boldsymbol{\xi}_k - \mathbb{E} \boldsymbol{\xi}_k^\top \mathbf{C} \boldsymbol{\xi}_k\right| \geq u \alpha^2 \|\mathbf{y} - \mathbf{y}'\|_2\right) \\ &\leq 4 \exp\left(-c m \min\left(\frac{u q}{\sqrt{2}}, \frac{u^2 q}{2}\right)\right). \end{aligned}$$

3. For $u > 0$,

$$\begin{aligned} &\Pr\left(H(\mathbf{y} - \mathbf{y}') \geq u \alpha \sqrt{\mathcal{M}^2 + 1} \|\mathbf{y} - \mathbf{y}'\|_2\right) \\ &= \Pr\left(H(\mathbf{y} - \mathbf{y}')^2 - \|\mathbf{y} - \mathbf{y}'\|_2^2 \geq (u^2 \alpha^2 (\mathcal{M}^2 + 1) - 1) \|\mathbf{y} - \mathbf{y}'\|_2^2\right) \quad (65) \\ &\leq \Pr\left(|H(\mathbf{y} - \mathbf{y}')^2 - \|\mathbf{y} - \mathbf{y}'\|_2^2| \geq (u^2 \alpha^2 - 1) (\mathcal{M}^2 + 1) \|\mathbf{y} - \mathbf{y}'\|_2^2\right). \end{aligned}$$

Since the two random variables H and Q have the relationship, $H(\mathbf{y} - \mathbf{y}')^2 - \|\mathbf{y} - \mathbf{y}'\|_2^2 = Q(\mathbf{y} - \mathbf{y}')$, continue from (65),

$$\Pr\left(H(\mathbf{y} - \mathbf{y}') \geq u \alpha \sqrt{\mathcal{M}^2 + 1} \|\mathbf{y} - \mathbf{y}'\|_2\right) \leq \Pr\left(|Q(\mathbf{y} - \mathbf{y}')| \geq (u^2 \alpha^2 - 1) (\mathcal{M}^2 + 1) \|\mathbf{y} - \mathbf{y}'\|_2^2\right).$$

We apply (33) to the vector $\frac{\mathbf{y}-\mathbf{y}'}{\|\mathbf{y}-\mathbf{y}'\|_2} \in \mathcal{S}^{n_1 n_2 - 1}$ and choose u to be $\frac{u^2 \alpha^2 - 1}{\alpha^2}$, we then have

$$\begin{aligned} \Pr \left(H(\mathbf{y} - \mathbf{y}') \geq u \alpha \sqrt{\mathcal{M}^2 + 1} \|\mathbf{y} - \mathbf{y}'\|_2 \right) &\leq \Pr \left(\left| Q \left(\frac{\mathbf{y} - \mathbf{y}'}{\|\mathbf{y} - \mathbf{y}'\|_2} \right) \right| \geq (u^2 \alpha^2 - 1) (\mathcal{M}^2 + 1) \right) \\ &\leq 4 \exp \left(-c m \min \left(\frac{u^2 \alpha^2 - 1}{\alpha^2} q, \left(\frac{u^2 \alpha^2 - 1}{\alpha^2} \right)^2 q \right) \right) \\ &= 4 \exp \left(-c m \frac{u^2 \alpha^2 - 1}{\alpha^2} q \right) \leq 4 \exp \left(-c m \frac{u^2 q}{1 + \frac{1}{\alpha^2}} \right), \quad \text{if } u \geq \sqrt{1 + \frac{1}{\alpha^2}}. \end{aligned}$$

The proofs for the three cases are complete. \square

D Proof of Lemma 4.3

The proof uses the standard generic chaining technique that relies on a smart construction of an admissible sequence defined as follows.

Definition D.1. Consider a metric space (T, d) , an admissible sequence of T is a collection of subsets of T , $\{T_s : s \in \mathbb{N}\}$, such that for every $s \geq 1$, $|T_s| \leq 2^{2^s}$ and $|T_0| = 1$. We then define a collection of maps: $\pi_s : T \rightarrow T_s$, where $\pi_s(t)$ is a nearest point to t with respect to the metric d .

In the following, we introduce the sub-Gaussian complexity: γ_2 -functional.

Definition D.2. Consider a metric space (T, d) , we define the γ_2 -functional by

$$\gamma_2(T, d) = \inf \sup_{t \in T} \sum_{s=0}^{\infty} 2^{\frac{s}{2}} d(t, T_s), \quad (66)$$

where $d(t, T_s)$ is the distance between the set T_s and t under certain metric.

In our analysis, we use the ℓ_2 norm in the Euclidean space as the metric d . For simplicity, we use $\gamma_2(\mathcal{Y})$ to denote $\gamma_2(\mathcal{Y}, \|\cdot\|_2)$. We first prove that the projection error $H(\mathbf{y} - \pi(\mathbf{y}))$ is bounded by $\gamma_2(\mathcal{Y})$ and then use the Talagrand majorizing measure theorem [42] to transform the dependence on γ_2 -functional to the Gaussian width $\mathbb{W}(\mathcal{Y})$.

Proof of Lemma 4.3. **1. The chaining set-up**

We begin proving Lemma 4.3. Fix $\mathcal{Y} \in \mathcal{S}^{n_1 n_2 - 1}$. Let $\{\mathcal{Y}_s : s \in \mathbb{N}\}$ be an admissible sequence of \mathcal{Y} such that

$$\gamma_2(\mathcal{Y}) \leq \sup_{\mathbf{y} \in \mathcal{Y}} \sum_{s=0}^{\infty} 2^{\frac{s}{2}} \|\pi_s(\mathbf{y}) - \mathbf{y}\|_2 \leq \gamma_2(\mathcal{Y}) + \frac{\gamma_2(\mathcal{Y})}{2} = \frac{3}{2} \gamma_2(\mathcal{Y}).$$

Then for every $\mathbf{y} \in \mathcal{Y}$,

$$\sum_{s=0}^{\infty} 2^{\frac{s}{2}} \|\pi_{s+1}(\mathbf{y}) - \pi_s(\mathbf{y})\|_2 \leq \sum_{s=0}^{\infty} 2^{\frac{s}{2}} (\|\pi_{s+1}(\mathbf{y}) - \mathbf{y}\|_2 + \|\pi_s(\mathbf{y}) - \mathbf{y}\|_2) \leq 3 \gamma_2(\mathcal{Y}). \quad (67)$$

We consider the relative end part of the chain. Let s_0 be the minimal integer such that $2^{s_0} > m$, implying $2^{s_0} \leq 2m$ and $|\mathcal{Y}_{s_0}| = 2^{2^{s_0}} \leq 2^{2m} = 4^m$.

From the definition of γ_2 functional in (66), $\lim_{s \rightarrow \infty} 2^{\frac{s}{2}} \|\pi_s(\mathbf{y}) - \mathbf{y}\|_2 = 0$, implying $\lim_{s \rightarrow \infty} \|\pi_s(\mathbf{y}) - \mathbf{y}\|_2 = 0$, so the sequence $\pi(\mathbf{y})$ converges to \mathbf{y} . Therefore we can write $\mathbf{y} - \pi_{s_0}(\mathbf{y}) = \sum_{s=s_0}^{\infty} \pi_{s+1}(\mathbf{y}) - \pi_s(\mathbf{y})$. Due to the sub-additivity of the function H ,

$$H(\mathbf{y} - \pi_{s_0}(\mathbf{y})) \leq \sum_{s=s_0}^{\infty} H(\pi_{s+1}(\mathbf{y}) - \pi_s(\mathbf{y})).$$

2. Controlling the increments

Set a scalar $\rho > 0$ to be

$$\rho = \max(\sqrt{2}, 4\sqrt{\frac{2}{c}}) \geq \max(\sqrt{1 + \frac{1}{\alpha^2}}, 4\sqrt{\frac{1 + \frac{1}{\alpha^2}}{c}}), \quad (68)$$

recalling $\alpha \geq 1$ in ⁵.

For $s \geq s_0$, fix two vectors $\mathbf{y}_s \in \mathcal{Y}_s, \mathbf{y}_{s+1} \in \mathcal{Y}_{s+1}$. Due to $2^{\frac{s}{2}} \geq 2^{\frac{s_0}{2}} > \sqrt{m}$, $\rho \frac{2^{\frac{s}{2}}}{\sqrt{m}} > \sqrt{1 + \frac{1}{\alpha^2}}$, we apply the result (35) in Lemma 4.2,

$$\begin{aligned} & \Pr \left(H(\mathbf{y}_{s+1} - \mathbf{y}_s) > \left(\rho \frac{2^{\frac{s}{2}}}{\sqrt{m}q} \right) \alpha \sqrt{\mathcal{M}^2 + 1} \|\mathbf{y}_{s+1} - \mathbf{y}_s\|_2 \right) \\ & \leq 4 \exp \left(-c m q \frac{\rho^2 \frac{2^s}{m} q}{1 + \frac{1}{\alpha^2}} \right) = 4 \exp \left(-c 2^s \frac{\rho^2}{1 + \frac{1}{\alpha^2}} \right). \end{aligned} \quad (69)$$

We then define the event E_s :

$E_s = \{ \text{there exist vectors } \mathbf{a} \in \mathcal{Y}_s, \mathbf{b} \in \mathcal{Y}_{s+1}, \text{ such that}$

$$H(\mathbf{a} - \mathbf{b}) > \left(\rho \frac{2^{\frac{s}{2}}}{\sqrt{m}q} \right) \alpha \sqrt{\mathcal{M}^2 + 1} \|\mathbf{a} - \mathbf{b}\|_2 \}.$$

Hence

$$E_s \subseteq \bigcup_{\substack{\mathbf{y}_{s+1} \in \mathcal{Y}_{s+1} \\ \mathbf{y}_s \in \mathcal{Y}_s}} \left\{ H(\mathbf{y}_{s+1} - \mathbf{y}_s) > \left(\rho \frac{2^{\frac{s}{2}}}{\sqrt{m}q} \right) \alpha \sqrt{\mathcal{M}^2 + 1} \|\mathbf{y}_{s+1} - \mathbf{y}_s\|_2 \right\}.$$

And there are at most $2^{2^s} 2^{2^{s+1}} = 2^{3 \cdot 2^s}$ pairs of $\mathbf{y}_s \in \mathcal{Y}_s$ and $\mathbf{y}_{s+1} \in \mathcal{Y}_{s+1}$, and $2^{3 \cdot 2^s} < 2^{2^{s+2}}$, thus we take a union bound by multiplying $2^{2^{s+2}}$ with the probability bound for one fixed pair $\mathbf{y}_s, \mathbf{y}_{s+1}$ given in (69), we can obtain

$$\begin{aligned} \Pr(E_s) & < 2^{2^{s+2}} 4 \exp \left(-c 2^s \frac{\rho^2}{1 + \frac{1}{\alpha^2}} \right) = 2^{2^{s+2}+2} \exp \left(-c 2^s \frac{\rho^2}{1 + \frac{1}{\alpha^2}} \right) \\ & < 2^{s+3} \exp \left(-c 2^s \frac{\rho^2}{1 + \frac{1}{\alpha^2}} \right) < \exp \left(2^{s+3} - c 2^s \frac{\rho^2}{1 + \frac{1}{\alpha^2}} \right) \leq \exp \left(-c 2^{s-1} \cdot \frac{\rho^2}{1 + \frac{1}{\alpha^2}} \right). \end{aligned}$$

In the last equality we use the fact $2^{s+3} \leq c 2^{s-1} \frac{\rho^2}{1+\frac{1}{\alpha^2}}$, which is a consequence of (68).

3. Summing up the increments

We define another event

$$E = \left\{ \text{there exists vector } \mathbf{z} \in \mathcal{Y} \text{ such that} \right. \\ \left. H(\mathbf{z} - \pi_{s_0}(\mathbf{z})) > \rho \alpha \sqrt{\mathcal{M}^2 + 1} \sum_{s=s_0}^{\infty} \frac{2^s}{\sqrt{m q}} \|\pi_{s+1}(\mathbf{z}) - \pi_s(\mathbf{z})\|_2 \right\}.$$

For any vector $\mathbf{y} \in \mathcal{Y}$, since $\pi_{s+1}(\mathbf{y}) \in \mathcal{Y}_{s+1}$ and $\pi_s(\mathbf{y}) \in \mathcal{Y}_s$, $E \subseteq \bigcup_{s=s_0}^{\infty} E_s$, and

$$\Pr(E) \leq \sum_{s=s_0}^{\infty} \Pr(E_s) \leq \sum_{s=s_0}^{\infty} \exp\left(-c 2^{s-1} \frac{\rho^2}{1+\frac{1}{\alpha^2}}\right). \quad (70)$$

We use the following exponential geometric series inequality to further bound the probability.

Lemma D.1. *Let $s_0 \in \mathbb{N}^+$ and a constant $L \geq 1$, then*

$$\sum_{s=s_0}^{\infty} \exp(-L 2^s) \leq \exp(-L 2^{s_0-1}).$$

By setting $L = c 2^{-1} \frac{\rho^2}{1+\frac{1}{\alpha^2}} > 1$, (see ρ set in (68)),

$$\Pr(E) \leq \sum_{s=s_0}^{\infty} \exp\left(-c 2^{s-1} \frac{\rho^2}{1+\frac{1}{\alpha^2}}\right) \\ \leq \exp\left(-c 2^{s_0-2} \frac{\rho^2}{1+\frac{1}{\alpha^2}}\right) \leq \exp(-2^{s_0+2}) < \exp(-4m). \quad (71)$$

The last line of derivations are due to $\frac{c\rho^2}{1+\frac{1}{\alpha^2}} \geq 2^4$ from (68), and s_0 satisfies $2^{s_0} > m$.

Since $\sup_{\mathbf{y} \in \mathcal{Y}} \sum_{s=s_0}^{\infty} 2^{\frac{s}{2}} \|\pi_{s+1}(\mathbf{y}) - \pi_s(\mathbf{y})\|_2 \leq 3\gamma_2(\mathcal{Y})$, the inclusion is as follows,

$$\left\{ \sup_{\mathbf{y} \in \mathcal{Y}} H(\mathbf{y} - \pi_{s_0}(\mathbf{y})) > \rho \alpha \sqrt{\mathcal{M}^2 + 1} \frac{3\gamma_2(\mathcal{Y})}{\sqrt{m q}} \right\} \\ \subseteq \left\{ \sup_{\mathbf{y} \in \mathcal{Y}} H(\mathbf{y} - \pi_{s_0}(\mathbf{y})) > \rho \alpha \sqrt{\mathcal{M}^2 + 1} \sup_{\mathbf{y} \in \mathcal{Y}} \sum_{s=s_0}^{\infty} \frac{2^{\frac{s}{2}}}{\sqrt{m q}} \|\pi_{s+1}(\mathbf{y}) - \pi_s(\mathbf{y})\|_2 \right\} \subseteq E.$$

From (71),

$$\Pr\left(\sup_{\mathbf{y} \in \mathcal{Y}} H(\mathbf{y} - \pi_{s_0}(\mathbf{y})) > \rho \alpha \sqrt{\mathcal{M}^2 + 1} \frac{3\gamma_2(\mathcal{Y})}{\sqrt{m q}}\right) < \exp(-4m). \quad (72)$$

4. Transforming γ_2 -functional to Gaussian width

In order to transform the γ_2 -functional to the Gaussian width \mathbb{W} , the final part is applying the Talagrand majorizing measure theorem [42].

Lemma D.2. *There exists a universal constant $\tilde{c} > 0$, for any set \mathcal{Y} ,*

$$\tilde{c} \gamma_2(\mathcal{Y}, \|\cdot\|_2) \leq \mathbb{W}(\mathcal{Y}) = \mathbb{E}_{\mathbf{n}} \sup_{\mathbf{y} \in \mathcal{Y}} \langle \mathbf{n}, \mathbf{y} \rangle.$$

Proof. Lemma D.2 is a special case of Theorem 5.1 in [42]. In particular, we treat the inner product $\langle \mathbf{n}, \mathbf{y} \rangle$ in the definition of $\mathbb{W}(\mathcal{Y})$ as a Gaussian process $X_{\mathbf{y}}$ indexed by the set \mathcal{Y} and choose the ℓ_2 distance as the metric for γ_2 due to $\|X_{\mathbf{y}} - X_{\mathbf{y}'}\|_2 = \mathbb{E} \langle \mathbf{n}, \mathbf{y} - \mathbf{y}' \rangle = \|\mathbf{y} - \mathbf{y}'\|_2$. \square

We set a universal constant

$$C' = \frac{\max(3\sqrt{2}, 12\sqrt{\frac{2}{\tilde{c}}})}{\tilde{c}} = \frac{3\rho}{\tilde{c}},$$

then $C' \mathbb{W}(\mathcal{Y}) \geq 3\rho \gamma_2(\mathcal{Y})$, and we apply the result given in (72),

$$\begin{aligned} & \Pr \left(\sup_{\mathbf{y} \in \mathcal{Y}} H(\mathbf{y} - \pi_{s_0}(\mathbf{y})) \leq C' \alpha \sqrt{\mathcal{M}^2 + 1} \frac{\mathbb{W}(\mathcal{Y})}{\sqrt{mq}} \right) \\ & \geq \Pr \left(\sup_{\mathbf{y} \in \mathcal{Y}} H(\mathbf{y} - \pi_{s_0}(\mathbf{y})) \leq 3\rho \alpha \sqrt{\mathcal{M}^2 + 1} \frac{\gamma_2(\mathcal{Y}, \|\cdot\|_2)}{\sqrt{mq}} \right) > 1 - \exp(-4m). \end{aligned}$$

By setting $\mathcal{Y}' = \mathcal{Y}_{s_0}$, $\pi = \pi_{s_0}$, we can conclude that for a positive integer m , there is a subset \mathcal{Y}' of $\mathcal{Y} \subset \mathcal{S}^{n_1 n_2 - 1}$ with cardinality less than 4^m , such that for every $\mathbf{y} \in \mathcal{Y}$, the projection error from \mathcal{Y} to \mathcal{Y}' under the formulation of H can achieve

$$\sup_{\mathbf{y} \in \mathcal{Y}} H(\mathbf{y} - \pi(\mathbf{y})) \leq C' \alpha \sqrt{\mathcal{M}^2 + 1} \frac{\mathbb{W}(\mathcal{Y})}{\sqrt{mq}}$$

with probability more than $1 - \exp(-4m)$, where C' is chosen to be $\frac{\max(3\sqrt{2}, 12\sqrt{\frac{2}{\tilde{c}}})}{\tilde{c}}$. \square

E Proof of Lemma 4.4

The proof also involves with the chaining method and follows similar steps in the previous proof for Lemma 4.3.

Proof. Fix a subset $\mathcal{Y}' \subset \mathcal{Y} \subset \mathcal{S}^{n_1 n_2 - 1}$ such that $|\mathcal{Y}'| \leq 4^m$. Similar to (67), let $\{\mathcal{Y}_s : s \in \mathbb{N}\}$ be an admissible sequence of \mathcal{Y}' such that

$$\sup_{\mathbf{y} \in \mathcal{Y}'} \sum_{s=0}^{\infty} 2^{\frac{s}{2}} \|\pi_{s+1}(\mathbf{y}) - \pi_s(\mathbf{y})\|_2 \leq 3 \gamma_2(\mathcal{Y}'). \quad (73)$$

Different from the proof of Lemma 4.3, we focus on the relative early part of the chain in this proof. We cut this beginning sequence into two pieces. Let s_0 be the minimal integer such that $2^{s_0} > 2m$ and fix an integer $0 \leq s_1 < s_0$. Then from Definition D.1, $\mathcal{Y}_{s_0} = \mathcal{Y}'$ ($|\mathcal{Y}'| \leq 4^m$) and we have $\mathbf{y} = \pi_{s_0}(\mathbf{y})$ for every $\mathbf{y} \in \mathcal{Y}'$. Hence,

$$Q(\mathbf{y}) = Q(\pi_{s_0}(\mathbf{y})) = \left(\sum_{s=s_1+1}^{s_0} Q(\pi_s(\mathbf{y})) - Q(\pi_{s-1}(\mathbf{y})) \right) + Q(\pi_{s_1}(\mathbf{y})).$$

Thus

$$\begin{aligned} \sup_{\mathbf{y} \in \mathcal{Y}'} |Q(\mathbf{y})| &\leq \sup_{\mathbf{y} \in \mathcal{Y}'} \left| \sum_{s=s_1+1}^{s_0} Q(\pi_s(\mathbf{y})) - Q(\pi_{s-1}(\mathbf{y})) \right| + \sup_{\mathbf{y} \in \mathcal{Y}'} |Q(\pi_{s_1}(\mathbf{y}))| \\ &\leq \sup_{\mathbf{y} \in \mathcal{Y}'} \left| \sum_{s=s_1+1}^{s_0} Q(\pi_s(\mathbf{y})) - Q(\pi_{s-1}(\mathbf{y})) \right| + \sup_{\mathbf{z} \in \mathcal{Y}_{s_1}} |Q(\mathbf{z})|. \end{aligned} \tag{74}$$

We proceed to respectively bound both supremums on the right side of (74).

1. For an integer $1 \leq s_1 + 1 \leq s \leq s_0$ and fixed $\mathbf{y}_s \in \mathcal{Y}_s, \mathbf{y}_{s-1} \in \mathcal{Y}_{s-1}$, by setting

$$\kappa = \max\left(2q, \frac{2^4}{c}\right) \quad \text{and} \quad u = \frac{\kappa}{q} \sqrt{\frac{2^s}{m}},$$

we apply the result in (34),

$$\begin{aligned} \Pr \left(|Q(\mathbf{y}_s) - Q(\mathbf{y}_{s-1})| > \frac{\kappa}{q} \alpha^2 (\mathcal{M}^2 + 1) \sqrt{\frac{2^s}{m}} \|\mathbf{y}_s - \mathbf{y}_{s-1}\|_2 \right) \\ \leq 4 \exp \left(-cm \min \left(\frac{\kappa}{\sqrt{2}} \sqrt{\frac{2^s}{m}}, \frac{\kappa^2}{2q} \frac{2^s}{m} \right) \right) = 4 \exp \left(-c \min \left(\frac{\kappa}{\sqrt{2}} \sqrt{2^s m}, \frac{\kappa^2}{2q} 2^s \right) \right). \end{aligned}$$

Because $2^{s-1} \leq 2^{s_0-1} \leq 2m$, the above inequality is further bounded by

$$\begin{aligned} 4 \exp \left(-c \min \left(\frac{\kappa}{\sqrt{2}} \sqrt{2^s 2^{s-2}}, \frac{\kappa^2}{2q} 2^s \right) \right) &\leq 4 \exp \left(-c \min \left(\frac{\kappa}{\sqrt{2}} 2^{s-1}, \frac{\kappa^2}{q} 2^{s-1} \right) \right) \\ &= 4 \exp \left(-c 2^{s-1} \min \left(\frac{\kappa}{\sqrt{2}}, \frac{\kappa^2}{q} \right) \right) \\ &= 4 \exp \left(-c 2^{s-1} \frac{\kappa}{\sqrt{2}} \right) < 4 \exp(-c 2^{s-2} \kappa), \end{aligned} \tag{75}$$

since $\kappa \geq \frac{q}{\sqrt{2}}$.

We define the event F_s :

$$\begin{aligned} F_s = \{ \text{there exist } \mathbf{c} \in \mathcal{Y}_s, \mathbf{d} \in \mathcal{Y}_{s-1} \text{ such that} \\ |Q(\mathbf{c}) - Q(\mathbf{d})| > \frac{\kappa}{q} \alpha^2 (\mathcal{M}^2 + 1) \sqrt{\frac{2^s}{m}} \|Q(\mathbf{c}) - Q(\mathbf{d})\|_2 \}. \end{aligned}$$

There are no more than $2^{2^{s+1}}$ pairs of $\mathbf{y}_s \in \mathcal{Y}_s$ and $\mathbf{y}_{s-1} \in \mathcal{Y}_{s-1}$, then we apply (75) and take a union bound for all possible pairs

$$\begin{aligned} \Pr(F_s) &\leq 2^{2^{s+1}} 4 \exp(-c 2^{s-2} \kappa) = 2^{2^{s+1}+2} \exp(-c 2^{s-2} \kappa) \\ &< 2^{2^{s+2}} \exp(-c 2^{s-2} \kappa) < \exp(2^{s+2} - 2^{s+3}), \quad \text{since } \kappa \geq \frac{2^5}{c} \\ &= \exp(-2^{s+2}). \end{aligned} \quad (76)$$

We then define another event

$$F = \left\{ \text{there exists some vector } \mathbf{z} \in \mathcal{Y}' \text{ such that} \right. \\ \left. \left| \sum_{s=s_1+1}^{s_0} Q(\pi_s(\mathbf{z})) - Q(\pi_{s-1}(\mathbf{z})) \right| > \frac{\kappa}{q} \alpha^2 (\mathcal{M}^2 + 1) \sum_{s=s_1+1}^{s_0} \sqrt{\frac{2^s}{m}} \|\pi_s(\mathbf{z}) - \pi_{s-1}(\mathbf{z})\|_2 \right\}.$$

We get to know that F belongs to $\bigcup_{s=s_1+1}^{s_0} F_s$, then from (76),

$$\Pr(F) \leq \sum_{s=s_1+1}^{s_0} \Pr(F_s) \leq \sum_{s=s_1+1}^{s_0} \exp(-2^{s+2}) \leq \exp(-2^{s_1+2}), \quad (77)$$

the last derivation is by Lemma D.1.

Recalling (73),

$$\sup_{\mathbf{y} \in \mathcal{Y}'} \sum_{s=s_1+1}^{s_0} 2^{\frac{s}{2}} \|\pi_s(\mathbf{y}) - \pi_{s-1}(\mathbf{y})\|_2 \leq 3 \gamma_2(\mathcal{Y}') \leq 3 \gamma_2(\mathcal{Y}),$$

thus by (77),

$$\begin{aligned} \Pr \left(\sup_{\mathbf{y} \in \mathcal{Y}'} \left| \sum_{s=s_1+1}^{s_0} Q(\pi_s(\mathbf{y})) - Q(\pi_{s-1}(\mathbf{y})) \right| > 3 \kappa \alpha^2 (\mathcal{M}^2 + 1) \frac{\gamma_2(\mathcal{Y})}{\sqrt{m} q} \right) \\ \leq \Pr(F) \leq \exp(-2^{s_1+2}), \quad \text{if } \kappa = \max\left(\frac{q}{\sqrt{2}}, \frac{2^5}{c}\right). \end{aligned} \quad (78)$$

2. Fix a vector $\mathbf{y}_{s_1} \in \mathcal{Y}_{s_1} \subset \mathcal{S}^{n_1 n_2 - 1}$, we apply (33) in Lemma 4.2, by setting $0 < u = \omega < 1$,

$$\begin{aligned} \Pr(|Q(\mathbf{y}_{s_1})| > \omega \alpha^2 (\mathcal{M}^2 + 1)) &\leq 4 \exp(-c m \min(\omega q, \omega^2 q)) \\ &= 4 \exp(-c m \omega^2 q). \end{aligned}$$

Then the supremum of $|Q(\cdot)|$ over the subset \mathcal{Y}_{s_1} satisfies

$$\begin{aligned} \Pr \left(\sup_{\mathbf{z} \in \mathcal{Y}_{s_1}} |Q(\mathbf{z})| > \omega \alpha^2 (\mathcal{M}^2 + 1) \right) \\ \leq |\mathcal{Y}_{s_1}| 4 \exp(-c m \omega^2 q) = 2 \cdot 2^{2^{s_1+1}} \exp(-c m \omega^2 q) \\ \leq 2 \cdot 2^{2^{s_1+1}} \exp(-c m \omega^2 q) < 2 \exp(2^{s_1+1} - c m \omega^2 q). \end{aligned} \quad (79)$$

Now recalling (74), we take a union bound for the probability of $\sup_{\mathbf{y} \in \mathcal{Y}'} |Q(\mathbf{y})|$ exceeding a distortion threshold by combining the results from (78) in part 1 and (79) in part 2,

$$\begin{aligned} & \Pr \left(\sup_{\mathbf{y} \in \mathcal{Y}'} |Q(\mathbf{y})| > \alpha^2 (\mathcal{M}^2 + 1) \left(3\kappa \frac{\gamma_2(\mathcal{Y})}{\sqrt{m}q} + \omega \right) \right) \\ & \leq \exp(-2^{s_1+2}) + 2 \exp(2^{s_1+1} - cm\omega^2 q), \quad \text{if } 0 < \omega < 1. \end{aligned} \quad (80)$$

If we choose s_1 to be the largest integer (can be 0) satisfying $s_1 < s_0$ and $2^{s_1+1} \leq cm \frac{\omega^2 q}{2}$, then

$$\exp(-2^{s_1+2}) < \exp\left(-cm \frac{\omega^2 q}{2}\right), \quad 2 \exp(2^{s_1+1} - cm\omega^2 q) \leq 2 \exp\left(-cm \frac{\omega^2 q}{2}\right).$$

Continuing from (80),

$$\Pr \left(\sup_{\mathbf{y} \in \mathcal{Y}'} |Q(\mathbf{y})| > \alpha^2 (\mathcal{M}^2 + 1) \left(3\kappa \frac{\gamma_2(\mathcal{Y})}{\sqrt{m}q} + \omega \right) \right) \leq 3 \exp\left(-cm \frac{\omega^2 q}{2}\right).$$

Again we use Lemma D.2 to replace $\gamma_2(\mathcal{Y})$ with $\mathbb{W}(\mathcal{Y})$ and set a constant

$$C''' = \frac{\max(\frac{3}{\sqrt{2}}, \frac{96}{c})}{\tilde{c}} \geq \frac{\max(\frac{3q}{\sqrt{2}}, \frac{96}{c})}{\tilde{c}} = \frac{3\kappa}{\tilde{c}},$$

hence $C''' \mathbb{W}(\mathcal{Y}) \geq 3\kappa \gamma_2(\mathcal{Y})$.

To conclude, for a fixed subset \mathcal{Y}' with $|\mathcal{Y}'| \leq 4^m$ and if $0 < \omega < 1$, the supremum of $Q(\mathbf{y})$ is concentrated as

$$\begin{aligned} & \Pr \left(\sup_{\mathbf{y} \in \mathcal{Y}'} |Q(\mathbf{y})| \leq \alpha^2 (\mathcal{M}^2 + 1) \left(C''' \frac{\mathbb{W}(\mathcal{Y})}{\sqrt{m}q} + \omega \right) \right) \\ & \geq \Pr \left(\sup_{\mathbf{y} \in \mathcal{Y}'} |Q(\mathbf{y})| \leq \alpha^2 (\mathcal{M}^2 + 1) \left(3\kappa \frac{\gamma_2(\mathcal{Y})}{\sqrt{m}q} + \omega \right) \right) \geq 1 - 3 \exp\left(-cm \frac{\omega^2 q}{2}\right). \end{aligned}$$

The proof is complete. \square